Perturbation of canonical and non-canonical BMP signaling affects migration, polarity and dendritogenesis of mouse cortical neurons

Monika Saxena[1], Nitin Agnihotri[1] and Jonaki Sen[1*]

Author affiliation:

[1]Department of Biological Sciences and Bioengineering, Indian Institute of Technology Kanpur, Kanpur-208016, Uttar Pradesh, India

[*]Corresponding Author:

E-mail address: jonaki@iitk.ac.in

Tel: +91-512-259-4054

Summary:

Perturbation of canonical and non-canonical BMP signaling has distinct effects on migration, polarity and dendritic morphology of upper layer cortical neurons in the mouse.

Abstract:

Bone Morphogenetic Protein (BMP) signaling has been implicated in regulation of patterning of the forebrain and as a regulator of neurogenesis and gliogenesis in the mammalian cortex. However, its role in regulating other aspects of cortical development *in vivo* remains unexplored. We hypothesized that BMP signaling may regulate additional processes during the development of cortical neurons after observing the presence of active BMP signaling in a spatio-temporally dynamic pattern in the mouse cortex. Our investigation revealed that BMP signaling specifically regulates migration, polarity and the dendritic morphology of upper layer cortical neurons born at E15.5. On further dissection of the role of canonical and non-canonical BMP signaling in each of these processes, we found that migration of these neurons is regulated by both canonical and non-canonical BMP signaling. Their polarity however appears to be affected more strongly by canonical BMP signaling while dendritic branch formation appears to be somewhat more strongly affected by LIMK-mediated non-canonical BMP signaling.

Introduction:

The cerebral cortex in the mammalian brain is comprised of neurons arranged in six molecularly distinct layers, the formation of which takes place in an inside out manner. For example, the early-born neurons give rise to the lower layers (i.e. layer V and VI) while the late born neurons form the upper layers (i.e. layer II-IV) with an exception of layer I, which comprises of the earliest born Cajal-Retzius cells (Angevine and Sidman, 1961, Rakic, 1974, Marín-Padilla, 1998).

The diverse population of projection neurons in the cortex are generated from the neural progenitors present in the ventricular zone (VZ) and the sub-ventricular zone (SVZ). Radial glia (RG) are a major class of neuronal progenitors that have long processes extending from the VZ to the pial surface which provide support to migrating neurons. RG undergo asymmetric

cell division giving rise to daughter radial glia as well as intermediate progenitors (IPs), which in turn undergo symmetric cell division to give rise to new born neurons (Noctor et al., 2004). These new born neurons, migrate through the SVZ to the intermediate zone (IZ), where they acquire a bipolar shape to start the process of radial migration (Tabata and Nakajima, 2003). The new born neurons destined to populate the lower layers undergo glia-independent somal translocation while upper layer neurons undergo glia-dependent radial migration (Nadarajah and Parnavelas, 2002, Nadarajah et al., 2001). When the migrating neurons reach the cortical plate (CP), the leading process transforms into the apical dendritic arbour projecting towards the pia, while the trailing process is converted into the prospective axon (Hatanaka and Murakami, 2002).

Several signaling pathways have been implicated in regulating different aspects of cortex development. For example, Fibroblast growth factors and Wnt proteins, have been implicated in regulation of patterning and proliferation of cortical progenitors. (Raballo et al., 2000, Chenn and Walsh, 2002, Woodhead et al., 2006). Notch signaling has been shown to be important for maintenance of the RG population in the VZ (Gaiano et al., 2000). In addition, Reelin (O'Dell et al., 2012, Jossin and Cooper, 2011, Franco et al., 2011) and retinoic acid (Choi et al., 2014, Siegenthaler et al., 2009) are known to regulate the layer specific positioning of migrating neurons.

In addition to the signaling molecules mentioned above, Bone Morphogenetic Proteins (BMPs), have been implicated in regulation of development of the central nervous system (Kalyani et al., 1998, Liem et al., 1995). Studies carried out with dissociated cortical cells or with cortical explants suggest that BMPs regulate cell proliferation, apoptosis and neuronal differentiation of cortical progenitors (Li et al., 1998, Mabie et al., 1999). In addition, BMPs are also known to regulate differentiation of astrocytes and parvalbulmin-positive interneurons (Bonaguidi et al., 2005, Gross et al., 1996, Mukhopadhyay et al., 2009). Although BMPs and

their receptors are expressed in the developing mouse forebrain from early stages (Furuta et al., 1997, Zhang et al., 1998, Caronia et al., 2010, Segklia et al., 2012)), the exploration of the role of BMP signaling *in vivo* in this context has been limited to studies demonstrating its role in dorso-medial patterning (Furuta et al., 1997, Hebert et al., 2002, Shimogori et al., 2004). The BMP receptor knockout mice had severe defects in early patterning of the forebrain, which precluded the exploration of possible other roles played by BMP signaling at later stages during cortical development.

To investigate the role of BMP signaling in the developing mouse cortex, we first detected the presence of active BMP signaling in the cortex at different developmental time points when cortical neurogenesis is going on. We observed a dynamic layer-specific activity of BMP signaling in the cortex, based on which we hypothesized that BMP signaling is likely to regulate other aspects of cortical development besides regulation of patterning and differentiation of astrocytes and interneurons. There is redundancy among multiple BMP ligands and receptors expressed in the mouse cortex (Caronia et.al., 2010; Furuta et al., 1997), hence complete abrogation of BMP signaling through genetic means in this context is difficult if not impossible. Thus to investigate the possible additional roles of BMP signaling in the developing mouse cortex, we adopted an *in utero* electroporation based strategy. We inhibited BMP signaling in a spatio-temporally regulated manner by delivering a dominant negative version of BMP receptor type 1b in the mouse cortex by *in utero* electroporation, followed by analysis at different developmental time points. Interestingly, we found that canonical and non-canonical BMP signaling seem to differentially regulate migration, polarity and dendritic branching of E15.5 born upper layer cortical neurons.

Result:

1. **Layer-specific BMP signaling observed during the course of development in the mouse cortex.**

In order to investigate the role of BMP signaling during cortical development in the mouse, we carried out a spatio-temporal analysis of active BMP signaling. Binding of BMP ligands to their cognate receptors leads to phosphorylation of the downstream effector molecule Smad1/5/8. Phosphorylated Smad1/5/8 (pSMAD1/5/8) enters into the nucleus with the help of the co-Smad, Samd4, to regulate the expression of the target genes of BMP signaling (Bandyopadhyay et al., 2013). Thus, to assess the presence of active BMP signaling in the developing mouse cortex, we carried out immunohistochemistry for pSMAD1/5/8 at embryonic day 11.5 and 15.5 (E11.5 and E15.5) and at postnatal days 0, 6 and 21 (P0, P6 and P21) (Figure 1). The pSMAD1/5/8 antibody used in this study has been previously demonstrated to specifically detect the presence of active BMP signaling in the context of the developing bone (Prashar et al., 2014). We observed the presence of active BMP signaling in distinct laminae within the cortex at different developmental stages. For instance, at E11.5, pSMAD1/5/8 is present in the ventricular zone (VZ), a niche for cortical progenitors (Figure 1B) and in the newly forming cortical preplate (PP), mostly comprising of post-mitotic neurons marked by Tbr1 (Figure 1B'). Similarly, at E15.5 pSMAD1/5/8 was detected in the VZ, in the sub-ventricular zone (SVZ), the IZ (Figure 1C) and in the cortical plate (CP) marked by Ctip2 expression (Figure 1C'). During later stages of cortex development at P0, pSMAD1/5/8 could be detected in all cortical laminae including the ones marked by Ctip2 expression, but at very low levels in the IZ and VZ-SVZ (Figure 1D). At postnatal day 6, pSMAD1/5/8 was observed mostly in the upper layers (Figure 1E, demarcated by dashed lines), marked by Brn2 expression (Figure 1E') and was also present in a mosaic pattern in the lower layers of the cortex (Figure 1E, white arrowheads). Finally, pSMAD1/5/8 immunoreactivity could be observed as late as

P21 in the upper layers of the cortex (Fig. 1F). Although, there is some background staining observed, especially in the meninges, the pSMAD1/5/8 immunostaining in the cortical neurons is specific, as it is present in the nucleus (Figure 1D and 1F, inset). These observations suggest that BMP signaling is active in the cortex in multiple laminae, across several developmental stages and hence, might be regulating distinct phenomena during the course of development.

2. Inhibition of BMP signaling affects the migration of E15.5 born upper layer cortical neurons in the mouse cortex.

To investigate the possible role(s) of BMP signaling during cortical development, we inhibited BMP signaling by overexpressing a dominant negative version of the BMP receptor 1b (dnBMPR1b), in the embryonic mouse cortex. Since dnBMPR1b lacks the entire intracellular region including the C-terminal serine-threonine kinase domain, when overexpressed, it competes with the endogenous type I BMP receptors, thus acting as a dominant negative (Kawakami et al., 1996) (Figure 2A).

We observed that pSMAD1/5/8 immunoreactivity was present in the cortical plate, SVZ and IZ at E15.5 and at P0 in all cortical layers. Based on this, we hypothesized that BMP signaling may significantly influence the development of cortical neurons in multiple layers. Thus, we chose the time points E13.5, E14.5 and E15.5 when both lower layer and upper layer neurons are born, to investigate the role of BMP signaling in their development. We used *in utero* electroporation to deliver a construct expressing dnBMPR1b (pCAG-dnBMPR1b) together with a GFP expressing construct (pCAG-GFP), in the mouse forebrain at E13.5, E14.5 and E15.5 (Fig. S1A and Fig. 2B). These animals will be henceforth referred to as test animals. Since pCAG-dnBMPR1b was co-electroporated with pCAG-GFP, majority of the GFP positive cells are expected to also express dnBMPR1b. We also electroporated pCAG-GFP alone in the mouse forebrain at all these stages which will henceforth be referred to as control animals.

The new born neurons generated from the progenitors in the VZ migrate through the SVZ to the lower part of the IZ. Our analysis of the cortex 48 hours after electroporation revealed that the distribution of GFP positive cells in the cortex of test animals electroporated at E15.5, was altered as compared to that in the control animals (Fig. 2C-D). However, there was no significant alteration in the distribution of GFP positive cells observed in the test animals electroporated at E13.5 and E14.5 compared to the control animals at these stages (Fig. S1B-G). When we analysed the cortices of the test and control animals, electroporated at E15.5, 48 hours after electroporation, we observed that in the test animals, there were considerable number of GFP positive cells still remaining in the SVZ and in the lower part of the IZ (Fig. 2D). However, in the control animals there were comparatively fewer GFP positive cells in the SVZ, most of them had migrated to the IZ and were well distributed there (Fig. 2C). On quantification of the number of GFP positive cells in the VZ-SVZ and the IZ, the difference in distribution of these cells between the test and control animals was found to be significant (Control: SVZ: 40.3 ± 3.13%; IZ: 59.6 ± 3.1% and test: SVZ: 65.2 ± 5.8%; IZ: 34.7 ± 5.8%; Fig. 2E).

To investigate the molecular nature of the GFP positive cells present in the SVZ in the test animals, we carried out immunohistochemical analysis for Tbr2, which mostly labels cells in the SVZ. We found a significant difference in the percentage of Tbr2-GFP double positive cells in the SVZ between the test and control animals (Fig. 2F-H, F' and G' white arrowheads) (Control: 44.8 ± 7.1%, dnBMPR1b: 70 ± 4%; Fig. 2H). Further, we analysed the effect of inhibition of BMP signaling on cell proliferation by quantifying the proportion of proliferating cells that have remained in the cell cycle 48 hours after labelling with EdU (see materials and methods). We found that in the dnBMPR1b electroporated cortex a greater proportion of the proliferating cells remained in the cell cycle as compared to the controls (Control: 20.6 ± 3.3%, dnBMPR1b: 35.6 ± 5.2%; Fig. 2J and S1H-I and I' white arrowheads). To assess the status of

BMP signaling in the GFP positive cells in test and control animals, we carried out immunohistochemical analysis for pSMAD1/5/8, which showed a significant decrease in the percentage of pSMAD1/5/8-GFP double positive cells in the test animals as compared to the controls (Control: 92.7 ± 2.5%, dnBMPR1b: 29.8 ± 0.8%; Fig. 2I).

When we analysed the effect of inhibition of BMP signaling in the cortices of mice at P0, in the animals that had been electroporated at E13.5 and E14.5, we found no significant difference in the distribution of GFP positive cells between the test and control animals (Fig. 3C-F). However, a striking effect of inhibition of BMP signaling was observed in the cortex of the test animals electroporated at E15.5 as compared to control. Majority of the GFP positive cells at this stage were found to be located in the IZ in the test animals whereas in control animals most of the GFP positive cells had migrated to the upper layer of the cortex (Fig. 3 G and H). To quantify the distribution of GFP positive cells across the cortex, we divided the cortical section into 7 equal bins with the bins 1-3 spanning the CP, bins 4 and 5 spanning the IZ and bins 6 and 7 corresponding to the SVZ and VZ respectively (Fig. 3I-K). In case of the animals electroporated at E13.5 and E14.5 there was no significant difference in the numbers of GFP positive cells across all the bins between the test and control animals (Fig. 3I and J). In contrast, in the animals electroporated at E15.5, we found the number of GFP positive cells present in bin1 to be significantly lower, whereas in bin 6 and 7, the number of GFP positive cells were significantly higher in test compared to control (Fig. 3K).

Moreover, we also observed a curious effect of inhibition of BMP signalling, on the morphology of the cells that seemed to be stuck in the IZ, in the cortex of the test animals. We observed a bifurcation in the leading process in many of the GFP positive cells in the test animals, while there was a single leading process in the cells at a comparable position in control animals (Compare Fig. 3G inset to 3H inset, white arrowheads and Fig 3N). Further, to ascertain whether there was significant downregulation of BMP signaling, we examined the

presence of pSMAD1/5/8 in GFP positive cells in the test and control animals. Immunohistochemical analysis revealed that majority of GFP positive neurons were negative for pSMAD1/5/8 in the cortical sections from test animals as compared to the cortical sections from the control animals (Fig. 3L, white arrowhead) (Control: 83.8 ± 0.7%, dnBMPR1b: 32.2 ± 1.4%; and Fig. 3M). Since we observed a migration defect as well as bifurcation of the leading process in the GFP positive cells in the test animals electroporated at E15.5 but not in those electroporated at E13.5 and E14.5, it appears that BMP signaling specifically regulates the migration of upper layer cortical neurons born at E15.5.

In order to verify that the observed differences in distribution of GFP positive cells in the VZ-SVZ and IZ, between the control and test, was not merely due to overexpression of BMP receptor 1b, we electroporated a construct expressing the full length BMPR1b at E15.5 and harvested the mice at E18.5. We observed that the distribution of GFP positive cells in the VZ, SVZ and the IZ in these cortical sections was very similar to that in the cortical sections from the control pCAG-GFP electroporated mouse (Fig 3O, Q and R). This indicated that the altered distribution of GFP positive cells observed in the dnBMPR1b electroporated mouse (Fig. 3P, asterisk and R) was specifically due to the inhibition of BMP signaling.

3. Inhibition of BMP signaling affects the polarity and dendritic branching of E15.5 born upper layer cortical neurons in the mouse cortex.

Our observation that inhibition of BMP signaling in the mouse cortex affected the migration of E15.5 born upper layer cortical neurons at P0, led us to further investigate if this is simply a delay in migration or a complete block in migration. For this, we examined the cortex of test and control animals at postnatal day 6 (P6), which had been electroporated at E15.5 (Fig. 4A-D). We found that in the cortical sections from test animals, there were

comparatively few GFP positive neurons which had migrated to the upper layer of the cortex. Moreover, the GFP positive neurons that had migrated in the test animals appeared to be disorganized and mis-aligned within the upper layer (Fig. 4B) as compared to those in the control animals (Fig. 4A). We also observed that in the test animals, the orientation of the cell body and the neuronal processes was disturbed in a significant number of GFP positive neurons, unlike that in the controls (compare Fig. 4A' to 4B'; Control: 9.5 ± 1.2%, dnBMPR1b: 64.9 ± 4.3%; Fig. 4F). To determine the layer-specific positioning of these GFP positive neurons in the cortex, we performed immunohistochemistry for Brn2, a marker of differentiated layer II/III cortical neurons (Fig. 4C and D). We observed that these GFP positive neurons express Brn2, suggesting that these neurons although disorganized and mis-oriented, had adopted the fate of layer II/III neurons even in the absence of BMP signaling (Fig. 4C' and D'). We found a significant decrease in pSMAD1/5/8 immunoreactivity in the GFP positive neurons in the test animals as compared to the controls indicating that BMP signaling is indeed downregulated (Fig.4G, white arrowheads; Control: 87.3 ± 2.6%, dnBMPR1b: 16.3 ± 3.1%; Fig. 4G').

In radially migrating neurons, the Golgi apparatus is localized to the leading process, which later on forms the apical dendrite of the differentiating neuron when it reaches the mantle zone. The localization of the Golgi in the leading process, determines the orientation of the apical dendrite of the differentiating neuron towards the pia of the cortex and thus imparts polarity to the neuron (Meseke et al., 2013, O'Dell et al., 2012, Matsuki et al., 2010). On inhibition of BMP signaling, we failed to observe a clearly distinguishable apical dendrite oriented towards the pia in GFP positive neurons. Thus, we wanted to ascertain, whether the Golgi apparatus was also mis-localized in these cells. We carried out immunohistochemistry for GM130, a Golgi protein, to localize the Golgi apparatus in the GFP positive neurons in the cortical sections from test and control animals at P6 (Fig. 4H, H' and supplementary movie 1

and Fig. 4I, I' and supplementary movie 2). We found that in majority of the GFP positive neurons from control animals, the Golgi is localized at the base of the apical dendrite and extending into it (referred to as cells with normal Golgi localization: 92.4±2.7%, Fig. 4L), and the cells are oriented towards the pia (Figure 4H, white arrowhead). In contrast, in the test animals, in a large proportion of the GFP positive neurons, the Golgi apparatus (Fig. 4I, white arrowheads) is distributed throughout the cytoplasm (referred to as cells with abnormal Golgi localization: 34.3±9.5%, Fig. 4L). Moreover, in these cells the dendritic processes were randomly oriented with no clearly distinguishable apical dendrite (Fig. 4I and I').

The mal-orientation of dendrites and the altered polarity of the GFP positive cortical neurons in the test animals prompted us to investigate the effect of inhibition of BMP signaling on formation of the dendritic arbour at a later time point. To study this, we analysed the GFP positive cells at postnatal day 15 (P15) in the cortex of test and control animals, which had been electroporated at E15.5. Although the apical dendrites in majority of the GFP positive neurons at this stage were found to be oriented towards the pia, the dendritic arbour of these neurons were much less elaborate in the cortical sections from test animals as compared to the control animals (compare Fig. 4J and K). We quantified the average number of branches emerging from GFP positive neurons in the test and control animals and we found that in the test animals the number of secondary as well as tertiary neurites (Fig. 4J and K, blue and green arrowheads) is significantly reduced (Fig. 4M). On the other hand, the primary neurites (Fig. 4J and K, red arrowheads) were not significantly reduced in number (Fig. 4M) in the test animals compared to the controls. Thus, BMP signaling seems to regulate the polarity of E15.5 born upper layer cortical neurons, which is manifested as Golgi mis-localization in the differentiating neuron at P6. In addition, BMP signalling also appears to be important for the formation of dendritic branches in these neurons at later stages.

4. BMP signaling regulates the migration of E15.5 born upper layer cortical neurons in the mouse through canonical as well as non-canonical pathways.

Bmps are known to signal through both canonical as well as non-canonical pathways. The canonical pathway involves phosphorylation of the downstream effector Smad1/5/8 and subsequent regulation of expression of Bmp target genes. There are several non-canonical pathways downstream of BMP, one of which results in activation of Lim kinase (LIMK) bound to the cytoplasmic tail of the type II BMP receptor. This is followed by phosphorylation of Cofilin by activated LIMK, ultimately, resulting in modulation of actin polymerization (Foletta et al., 2003). It has been reported through *in vitro* studies that the dendritogenesis of cortical neurons is regulated by BMP signaling acting through the non-canonical LIMK mediated pathway (Lee-Hoeflich et al., 2004). LIMK activation downstream of BMP signaling is dependent on the following two factors: 1) Binding of LIMK to the cytoplasmic domain of BMPRII, which relieves an auto-inhibitory effect on its catalytic domain (Lee-Hoeflich et al., 2004) and 2) Phosphorylation of the activation loop of LIMK by P21-activated kinase 1 (PAK1), which interacts with BMP receptor Type I (Podkowa et al., 2013) (Fig. 8). Thus we speculate that when we overexpressed the dominant negative type I BMP receptor, it led to blockage of canonical BMP signaling by inhibition of Smad1/5/8 phosphorylation and blockage of non-canonical BMP signaling by preventing the PAK1-mediated activation of LIMK (Fig. 8).

Since overexpression of dnBMPR1b in the developing mouse cortex led to defects in neuronal migration, polarity and dendritic morphology, we wanted to investigate the contribution of canonical and non-canonical BMP signaling to each of these observed phenotypes. To address this, we decided to selectively inhibit the Smad-dependent canonical pathway by overexpressing Smuf1, which is an E3 ubiquitin ligase for Smad proteins (Zhu et al., 1999). On the other hand, to inhibit the LIMK mediated non-canonical BMP pathway, we

overexpressed a BMP receptor type II lacking the LIMK interacting domain in its cytoplasmic tail (BMPRIIΔLIMK) (Phan et al., 2010) (Fig. 5A). In order to assess the efficiency of these constructs to selectively inhibit canonical and non-canonical BMP signaling, we co-transfected 293T cells with either pCAG-dnBMPR1b, pCAG-Smurf1 or pCAG-BMPRIIΔLIMK along with pCAG-GFP. This was followed by immunohistochemical detection of pSMAD1/5/8 and phosphorylated Cofilin (p-Cofilin) as readouts of the canonical and non-canonical pathways respectively (see supplementary materials and methods). We observed that the dnBMPR1b construct inhibited both canonical and non-canonical BMP signalling. On the other hand, the pCAG-BMPRIIΔLIMK and the pCAG- Smurf1 constructs, inhibited only the non–canonical or the canonical pathway respectively (Fig. S2A).

Subsequently, we co-electroporated either pCAG-Smurf1 or pCAG-BMPRIIΔLIMK together with pCAG-GFP, in the developing mouse cortex *in utero* at E15.5. The cortices from these animals were analysed at E17.5 (Fig. S2B-D, D') and P0 (Fig. 5), to study the effect, if any, on migration of upper layer neurons. We found that at E17.5, majority of GFP positive cells in the cortex overexpressing Smurf1, were stuck in the SVZ (Fig. S2C and D') similar to what was observed with dnBMPR1b overexpression (Fig. 2D). However, there was no obvious defect in the migration of GFP positive neurons in the cortex overexpressing BMPRIIΔLIMK (Fig. S2D and D') which was similar to the control (Fig. S2B).

When we analysed the cortex overexpressing Smurf1 and BMPRIIΔLIMK at P0, we found that many of the cortical neurons had failed to migrate to their final positions in both cases (Figure 5E and F, respectively), as compared to the pCAG-GFP electroporated control (Fig. 5C and 3G). However, the defect in migration of cortical neurons observed in the animals overexpression Smurf1 and BMPRIIΔLIMK, was less severe compared to that observed with overexpression of dnBMPR1b (Fig. 5D and 3H). In order to quantify the distribution of GFP positive neurons in each case, we divided the cortical section into 7 equal bins similar to that

shown in Figure 3I. We observed that in the cortex overexpressing both the Smurf1 and the BMPRIIΔLIMK, the number of GFP positive cells in bin1 was significantly lower than in the control animals, while it was relatively higher than that in the cortex overexpressing dnBMPR1b (Fig. 5G). On the other hand, we also found that in both the cases (cortices with overexpression of Smurf1 and BMPRIIΔLIMK) the number of GFP positive cells in bins 6-7 (encompassing VZ and SVZ) were significantly higher than that in the control, but only somewhat lower than that in the dnBMPR1b overexpressing cortical sections (Figure 5G).

Immunohistochemical analysis revealed a significant decrease in number of pSMAD1/5/8 positive cells in the cortices with overexpressing Smurf1 as compared to control (Fig. 5H and H', white arrowheads, Control: 83.4 ± 0.7%, Smurf1: 22 ± 5.5%; Fig. 5I). Similarly a significant decrease in p-Cofilin in the cortices overexpressing BMPRIIΔLIMK was observed as compared to the control (Fig. 5J and J', white arrowheads, Control: 95.9 ± 1.7%, BMPRIIΔLIMK: 23.5 ± 1.1%; Fig. 5K). We also noticed a bifurcation of the leading process in a few GFP positive cells in the cortex overexpressing either Smurf1 or BMPRIIΔLIMK, as previously observed in the cortex overexpressing dnBMPR1b (Fig. 5C-F insets, red arrowheads). Thus, these observations suggest that BMP signaling regulates the migration of E15.5 born upper layer cortical neurons through both canonical and LIMK mediated non-canonical pathways.

5. Canonical BMP signaling regulates polarity of E15.5 born upper layer pyramidal neurons of the mouse cortex.

We examined the cortices of the mice electroporated with pCAG-Smurf1 and pCAG-BMPRIIΔLIMK at P6, in order to determine the role of the canonical versus non-canonical BMP signaling in regulating the polarity of upper layer pyramidal neurons (Fig. 6). We found

that in majority of the GFP positive cells overexpressing Smurf1, the Golgi apparatus was mis-localized and distributed throughout the cytoplasm of the cell body (Fig. 6C, C' and C'', white arrowheads) and orientation of cell body is disturbed similar to what was observed in the GFP positive cells expressing dnbMPR1b (Fig. 6B, B' and B'' B, white arrowheads). On the other hand, in majority of the GFP positive cells overexpressing BMPRIIΔLIMK, the Golgi was localized correctly to the base of the apical dendrite and extending into it (Figure 6D, D' and D'', white arrowheads) similar to that observed in the control (Fig. 6 A, A' and A'', white arrowheads). The specific effect of inhibition of canonical BMP signaling on the polarity of the GFP positive cells became clearer on quantification (Fig. 6I). It is worth mentioning here that although a small proportion (16.3±2.8%) of GFP positive cells overexpressing BMPRIIΔLIMK did show mis-localization of the Golgi, this was significantly lower than that observed in either cells overexpressing dnBMPR1b (36.8±10.4%) or Smurf1 (40.6 ± 5.1%). We confirmed the downregulation of canonical and LIMK mediated non-canonical BMP signaling in the cortex overexpressing Smurf1 and BMPRIIΔLIMK respectively, by examining the level of pSMAD1/5/8 and p-Cofilin. We found a significant decrease in number of cells with pSMAD1/5/8 immunoreactivity among cells overexpressing Smurf1 as compared to control (Fig. 6E white arrowheads; Control: 87.3 ± 2.6 %, Smurf1: 20 ± 4.5 %;, Fig. 6F). Similarly we also found a significant decrease in number of cell with p-Cofilin immunoreactivity among the cells overexpressing BMPRIIΔLIMK as compared to control (Fig. 6G, white arrowheads; Control: 90.6 ± 1.6 %, BMPRIIΔLIMK: 20.4 ± 3 %; Fig. 6H). Thus, it appears that Smad dependent canonical BMP signaling is more critical than the non-canonical LIMK mediated BMP pathway for establishing the polarity of E15.5 born upper layer neurons.

6. **Non-canonical BMP signaling plays a major role in dendritogenesis of E15.5 born upper layer pyramidal neurons.**

We had previously observed that at P15, the upper layer pyramidal neurons expressing dnBMPR1b, had a reduced dendritic arbour with fewer secondary and tertiary branches. To investigate the effect of canonical and non-canonical BMP signaling on dendritogenesis, we extended this analysis to P21, when dendritogenesis has progressed further and the dendritic spines can be visualised. We found that at P21, there is a significant decrease in the number of primary neurites and a dramatic decrease in the number of secondary and tertiary neurites in the neurons overexpressing dnBMPR1b and BMPRIIΔLIMK as compared to the control (Fig. 7A, B and D; Fig. 7E-G). However, the decrease in the number of secondary and tertiary neurites was not significant in the Smurf1 overexpressing neurons as compared to the control (Fig. 7A, C and Fig. 7F and G). Upon quantifying the length of the dendritic branches we found a significant difference in the length of both primary and secondary neurites in the neurons overexpressing dnBMPR1b and BMPRIIΔLIMK compared to the control (Fig.7H and I). In the case of Smurf1 overexpressing neurons there seem to be a slight decrease in the length of primary neurites as compared to controls, but this decrease although significant as compared to control, was not as much as that observed with either dnBMPR1b or BMPRIIΔLIMK expressing neurons (Fig.7H).

Since the dendritic spines could be clearly distinguished at P21, we quantified the number of spines present per 10 µm of dendritic length. We found a significant decrease in the spine density in neurons overexpressing BMPRIIΔLIMK as compared to the control (compare Fig. 7M to 7J and the corresponding bars in Fig. 7N). The dnBMPR1b as well as the Smurf1 overexpressing neurons too exhibited a decreased spine density as compared to the control (compare Fig.7K and 7L to 7J and the corresponding bars in Fig. 7N). However, the decrease in spine density in the dnBMPR1b as well as the Smurf1 overexpressing neurons was not as

much as that observed with the neurons overexpressing BMPRIIΔLIMK. Thus, our observations suggest that dendritic branch formation of E15.5 born upper layer neurons is minimally affected by inhibition of canonical BMP signaling whereas it is severely affected by inhibition of LIMK mediated non-canonical BMP signaling.

Discussion:

This study has revealed a highly dynamic spatio-temporal pattern of canonical BMP signaling during the development of the cortex, strongly suggesting that this pathway regulates multiple aspects of cortical development. When we inhibited BMP signaling by overexpressing dnBMPR1b during cortical development we found that it affected migration, polarity and dendritic morphogenesis of E15.5 born upper layer cortical neurons. As dnBMPR1b inhibits both canonical and non-canonical BMP signaling we designed experiments to dissect the role of these two types of BMP signaling in each of the three observed phenotypes. Our data suggests that migration of E15.5 born upper layer cortical neurons is regulated by both pSMAD-mediated canonical and LIMK-mediated non-canonical BMP signaling. On the other hand, canonical BMP signaling seems to be the major regulator of polarity of these neurons, while the formation of dendritic branches seem to be mostly regulated by LIMK-mediated non-canonical BMP signaling (Fig. 8).

We observed that migration of the neurons that are born at E15.5 and mostly populate the upper cortical layers is specifically delayed upon overexpression of dnBMPR1b. On the other hand, the migration of the neurons that are born at E13.5 and E14.5 is largely unaffected upon inhibition of BMP signaling. Unlike the E13.5 born neurons which populate the lower cortical layers, the E14.5 and E15.5 born neurons populating the upper cortical layers (constituting layer IV and layer II-III respectively) undergo glial-dependent radial migration.

However, inhibition of BMP signaling seems to affect only the migration of the upper layer neurons born at E15.5 but not that of the neurons born at E14.5 neurons. This differential effect of BMP signaling on the migration of E15.5 born neurons is very interesting. It suggests that the migration of the E14.5 born upper layer neurons is independent of BMP signaling and may involve a separate set of molecular players.

One of the possible explanations for this effect on migration may be a delay in neurogenesis which results in a subsequent delay in migration. Indeed, when we examined the effect of inhibition of BMP signaling on cell proliferation at E17.5, we found that a greater proportion of the proliferating cells remained in the cell cycle in the dnBMPR1b electroporated cortex as compared to the control. This suggests that the delay in migration may occur due to a delay in neurogenesis. However, further experiments need to be carried out in order to determine if inhibition of BMP signaling is likely to affect the later stages of migration of upper layer cortical neurons that occur post-neurogenesis.

Subsequently, when we inhibited canonical BMP signaling by overexpressing Smurf1 or inhibited non-canonical BMP signaling by overexpressing BMPRIIΔLIMK in the mouse cortex, we did observe a delay in migration of these neurons, but the effect was not as dramatic as that observed with overexpression of dnBMPR1b. This indicates that both canonical and LIMK-mediated non-canonical BMP signaling are necessary for proper migration of E15.5 born upper layer neurons and explains the severity of the migration defect observed on expression of dnBMPR1b which inhibits both of these pathways (Fig. 8).

On inhibition of BMP signaling with overexpression of dnBMPR1b we also observed morphological changes such as the bifurcation of the leading process in the neurons that were stuck in the IZ during migration. A bifurcated leading process had been previously reported in neurons where modulators of RhoA activity have been knocked down (Pacary et al., 2011,

Azzarelli et al., 2014, Hand et al., 2005, Pacary et al., 2013). Thus, we speculate that BMP signaling may regulate the migration of E15.5 born upper layer cortical neurons through modulating RhoA activity.

At P6, we observed another effect of inhibition of BMP signalling, which is, an alteration in the polarity of the E15.5 born upper layer cortical neurons. This was manifested as an indistinguishable apical dendrite and mis-localization of the Golgi. We observed similar mis-localized Golgi in the neurons overexpressing Smurf1 but not in significant numbers in the neurons overexpressing BMPRIIΔLIMK. Though the process of establishment of cell polarity may involve cytoskeletal changes our data seems to indicate that the cytoskeletal changes orchestrated by non-canonical BMP signaling do not play a role in this process. This suggests that canonical BMP signaling is primarily required for polarity of the E15.5 born upper layer neurons (Fig. 8).

At P21 we observed a significant effect of inhibition of BMP signaling on dendritic morphology which included dendritic branching, length and spine density. The branching and length of dendrites was most significantly decreased in neurons where the LIMK-dependent non-canonical BMP signaling had been inhibited. In contrast, in neurons where canonical BMP signaling was selectively inhibited by Smurf1 overexpression, there was no significant change in dendritic branching or length as compared to the control. In case of spine density the maximum decrease was observed with inhibition of the LIMK-mediated non-canonical BMP signaling. This suggests that the effect of overexpression of dnBMPR1b on morphogenesis of dendrites is mostly a reflection of the inhibition of LIMK-mediated non-canonical BMP signaling (Fig. 8). Previous studies with cortical neurons *in vitro* have demonstrated that LIMK mediated non-canonical BMP signaling is a key regulator of dendritogenesis (Lee-Hoeflich et al., 2004), our study has provided *in vivo* data in support of this.

In conclusion, this study has yielded data in strong support of our hypothesis that BMP signaling is involved in regulating several diverse developmental phenomena in the mouse cortex. We found that inhibition of BMP signaling specifically affects the migration, establishment of polarity and dendritic morphogenesis of E15.5 born upper layer pyramidal neurons. In addition this study has also dissected out the contribution of canonical and LIMK-dependent non-canonical BMP signaling in regulating each of the above-mentioned phenotypes. Further exploration in future will identify the specific downstream effectors of BMP signaling that regulate each of the three above mentioned phenomena.

Material and Methods:

Experimental animals:

All animal experiments were performed according to the protocol sanctioned by Institute Animal Ethics Committee, registered with CPCSEA (Reg. no. 810/ 03/ ac/ CPCSEA, dated 15/10/2003). Wild type mice (CByB6F1/J, Stock no. 100009; The Jackson Laboratory) were crossed to generate timed pregnant females for the experiments.

In utero electroporation:

Timed pregnant females were anesthetized with the help of isoflurane vaporizer (Patterson Veterinary). Uterine horns of the pregnant female were exposed and the DNA corresponding to the desired construct(s) was injected at a total concentration of 1µg/µl along with 1% fast green dye into the forebrain of the embryos. Electroporation was performed with the tweezer-disc electrodes (LF650S10, Bex Co., LTD) providing an electric pulse of 35V for 50 milliseconds, five times at the interval of 950 milliseconds using the electroporator (ECM830, BTX, Harvard apparatus).

Constructs:

Following constructs were used in this study: (1) pCAG-GFP (a gift from Prof. Constance Cepko, Harvard Medical School, Boston, USA), (2) pCAG-dnBMPR1b, (3) pCAG-BMPRIIΔLIMK, (4) pCAG-Smurf1. See Supplementary information for constructs (2), (3) and (4).

Immunohistochemistry:

Mouse forebrain sections of desired stage were subjected to immunohistochemical experiment. The following primary antibodies were used: anti-pSMAD1/5/8 (1:100, Cat.no. 8828, Cell Signaling Technology), anti-Tbr1 (1:2000, Cat no. Ab31940, Abcam), anti-Tbr2 (1:1000, Cat no. Ab15894, Abcam), anti-Ctip2 (1:300, Cat no. Ab28448, Abcam) anti-Brn2 (1: 4000, Cat no. SC6029, Santa Cruz Biotechnology Inc.), anti p-Cofilin (1:300, Cat no. SC21867R, Santa Cruz Biotechnology Inc.), anti-GM130 (1:300, Cat no. 610822, BD Biosciences) and anti-GFP (1:500, Cat no. A-6455, ThermoFisher Scietific), anti-Ki67 (1:500, Cat. No. AB39260, Abcam). See Supplementary information for details.

Cell proliferation analysis:

The timed pregnant females were injected with EdU via intraperitoneal injection at the dose 20mg/kg of the body weight 2 hours before the *in utero* electroporation at E15.5 and embryos were harvested at E17.5 for analysis. EdU labelling in the electroporated cells in the cortical sections was detected by using Click-iT^{TM} EdU imaging kit (Cat. No. C10338). EdU-GFP double positive cells were further analysed for the presence of Ki67, a marker for proliferating cells by performing immunohistochemistry in the cortical section after EdU detection assay. The fraction of GFP positive cells that remain in cell cycle were estimated by counting the number of GFP-EdU-Ki67 triple positive cells among the GFP-EdU double positive cells.

Quantification:

For each quantification, GFP positive cells from three consecutive sections of an embryo were counted, averaged and considered as n =1. At least, three such embryos (n = 3) were analysed for each experiment. For quantification of dendritic branches, the average number of primary, secondary and tertiary branches were calculated for 50 GFP positive neurons per animal and this was considered as n = 1. Counting of GFP positive cells and dendritic branches was performed using ImageJ software. See supplementary information for details.

Imaging and morphological analysis:

Sections of the mouse cortex electroporated with the various constructs were imaged and analysed using the multiphoton laser scanning confocal microscope LSM780 (Carl Zeiss Inc.) and ZEN 2011 software. Neurite length was estimated by using the NeuronJ software (https://imagescience.org/meijering/software/neuronj), an ImageJ plugin for neurite tracing and the instructions provided in the manual were followed.

Statistical analysis:

Statistical analysed was performed for all data sets and data is represented as average mean ± standard deviation using Microsoft office excel software. The unpaired student's *t*-test was performed to analyse statistical significance (*p <0.05, **p <0.005, #p>0.05). One-way analysis of variance (ANOVA) was performed to compare the means of more than two groups and post-hoc analysis was performed by using two tailed student's *t*-test (Figure 4-6).

Acknowledgement: We are grateful to Dr. Amitabha Bandyopadhyay and Dr. Sandeep Gupta for their critical comments on the manuscript. We are also thankful to Mr. Ali Abbas Zaidi for his help in sub-cloning of dnBMPR1b, Mr. Tathagat Biswas for helping in preparation of movie files of GM130 immunostaining and Ms. Neetu Dey for her help with confocal imaging.

Competing interests: Authors have declared no competing interest.

Author Contributions: JS conceived the study, JS and MS designed the experiments, MS carried out all experiments. JS and MS analysed the data and wrote the manuscript. NA performed RNA in situ hybridization for dnBMPR1b and assisted in analysis.

Funding: This work was supported by Department of Biotechnology, Ministry of Science and Technology, New Delhi, India (Grant no. BT/PR1880/MED/30/624/2011 to JS). MS was supported by UGC, Govt. of India for her PhD fellowship. NA is supported by Ministry of Human Resources and Development, Govt. of India for his PhD fellowship.

References:

ANGEVINE, J. B., JR. & SIDMAN, R. L. 1961. Autoradiographic study of cell migration during histogenesis of cerebral cortex in the mouse. *Nature,* 192, 766-8.

AZZARELLI, R., PACARY, E., GARG, R., GARCEZ, P., VAN DEN BERG, D., RIOU, P., RIDLEY, A. J., FRIEDEL, R. H., PARSONS, M. & GUILLEMOT, F. 2014. An antagonistic interaction between PlexinB2 and Rnd3 controls RhoA activity and cortical neuron migration. *Nat Commun,* 5, 3405.

BANDYOPADHYAY, A., YADAV, P. S. & PRASHAR, P. 2013. BMP signaling in development and diseases: a pharmacological perspective. *Biochem Pharmacol,* 85, 857-64.

BONAGUIDI, M. A., MCGUIRE, T., HU, M., KAN, L., SAMANTA, J. & KESSLER, J. A. 2005. LIF and BMP signaling generate separate and discrete types of GFAP-expressing cells. *Development,* 132, 5503-14.

CARONIA, G., WILCOXON, J., FELDMAN, P. & GROVE, E. A. 2010. Bone morphogenetic protein signaling in the developing telencephalon controls formation of the hippocampal dentate gyrus and modifies fear-related behavior. *J Neurosci,* 30, 6291-301.

CHENN, A. & WALSH, C. A. 2002. Regulation of cerebral cortical size by control of cell cycle exit in neural precursors. *Science,* 297, 365-9.

CHOI, J., PARK, S. & SOCKANATHAN, S. 2014. Activated retinoid receptors are required for the migration and fate maintenance of subsets of cortical neurons. *Development,* 141, 1151-60.

FOLETTA, V. C., LIM, M. A., SOOSAIRAJAH, J., KELLY, A. P., STANLEY, E. G., SHANNON, M., HE, W., DAS, S., MASSAGUE, J. & BERNARD, O. 2003. Direct signaling by the BMP type II receptor via the cytoskeletal regulator LIMK1. *J Cell Biol,* 162, 1089-98.

FRANCO, S. J., MARTINEZ-GARAY, I., GIL-SANZ, C., HARKINS-PERRY, S. R. & MULLER, U. 2011. Reelin regulates cadherin function via Dab1/Rap1 to control neuronal migration and lamination in the neocortex. *Neuron,* 69, 482-97.

FURUTA, Y., PISTON, D. W. & HOGAN, B. L. 1997. Bone morphogenetic proteins (BMPs) as regulators of dorsal forebrain development. *Development,* 124, 2203-12.

GAIANO, N., NYE, J. S. & FISHELL, G. 2000. Radial glial identity is promoted by Notch1 signaling in the murine forebrain. *Neuron,* 26, 395-404.

GROSS, R. E., MEHLER, M. F., MABIE, P. C., ZANG, Z., SANTSCHI, L. & KESSLER, J. A. 1996. Bone morphogenetic proteins promote astroglial lineage commitment by mammalian subventricular zone progenitor cells. *Neuron,* 17, 595-606.

HAND, R., BORTONE, D., MATTAR, P., NGUYEN, L., HENG, J. I., GUERRIER, S., BOUTT, E., PETERS, E., BARNES, A. P., PARRAS, C., SCHUURMANS, C., GUILLEMOT, F. & POLLEUX, F. 2005. Phosphorylation of Neurogenin2 specifies the migration properties and the dendritic morphology of pyramidal neurons in the neocortex. *Neuron,* 48, 45-62.

HATANAKA, Y. & MURAKAMI, F. 2002. In vitro analysis of the origin, migratory behavior, and maturation of cortical pyramidal cells. *J Comp Neurol,* 454, 1-14.

HEBERT, J. M., MISHINA, Y. & MCCONNELL, S. K. 2002. BMP signaling is required locally to pattern the dorsal telencephalic midline. *Neuron,* 35, 1029-41.

JOSSIN, Y. & COOPER, J. A. 2011. Reelin, Rap1 and N-cadherin orient the migration of multipolar neurons in the developing neocortex. *Nat Neurosci,* 14, 697-703.

KALYANI, A. J., PIPER, D., MUJTABA, T., LUCERO, M. T. & RAO, M. S. 1998. Spinal cord neuronal precursors generate multiple neuronal phenotypes in culture. *J Neurosci,* 18, 7856-68.

KAWAKAMI, Y., ISHIKAWA, T., SHIMABARA, M., TANDA, N., ENOMOTO-IWAMOTO, M., IWAMOTO, M., KUWANA, T., UEKI, A., NOJI, S. & NOHNO, T. 1996. BMP signaling during bone pattern determination in the developing limb. *Development,* 122, 3557-66.

LEE-HOEFLICH, S. T., CAUSING, C. G., PODKOWA, M., ZHAO, X., WRANA, J. L. & ATTISANO, L. 2004. Activation of LIMK1 by binding to the BMP receptor, BMPRII, regulates BMP-dependent dendritogenesis. *EMBO J,* 23, 4792-801.

LI, W., COGSWELL, C. A. & LOTURCO, J. J. 1998. Neuronal differentiation of precursors in the neocortical ventricular zone is triggered by BMP. *J Neurosci,* 18, 8853-62.

LIEM, K. F., JR., TREMML, G., ROELINK, H. & JESSELL, T. M. 1995. Dorsal differentiation of neural plate cells induced by BMP-mediated signals from epidermal ectoderm. *Cell,* 82, 969-79.

MABIE, P. C., MEHLER, M. F. & KESSLER, J. A. 1999. Multiple roles of bone morphogenetic protein signaling in the regulation of cortical cell number and phenotype. *J Neurosci,* 19, 7077-88.

MARÍN-PADILLA, M. 1998. Cajal–Retzius cells and the development of the neocortex. *Trends in Neurosciences,* 21, 64-71.

MATSUKI, T., MATTHEWS, R. T., COOPER, J. A., VAN DER BRUG, M. P., COOKSON, M. R., HARDY, J. A., OLSON, E. C. & HOWELL, B. W. 2010. Reelin and stk25 have opposing roles in neuronal polarization and dendritic Golgi deployment. *Cell,* 143, 826-36.

MESEKE, M., ROSENBERGER, G. & FORSTER, E. 2013. Reelin and the Cdc42/Rac1 guanine nucleotide exchange factor alphaPIX/Arhgef6 promote dendritic Golgi translocation in hippocampal neurons. *Eur J Neurosci,* 37, 1404-12.

MUKHOPADHYAY, A., MCGUIRE, T., PENG, C. Y. & KESSLER, J. A. 2009. Differential effects of BMP signaling on parvalbumin and somatostatin interneuron differentiation. *Development,* 136, 2633-42.

NADARAJAH, B., BRUNSTROM, J. E., GRUTZENDLER, J., WONG, R. O. & PEARLMAN, A. L. 2001. Two modes of radial migration in early development of the cerebral cortex. *Nat Neurosci,* 4, 143-50.

NADARAJAH, B. & PARNAVELAS, J. G. 2002. Modes of neuronal migration in the developing cerebral cortex. *Nat Rev Neurosci,* 3, 423-32.

NOCTOR, S. C., MARTINEZ-CERDENO, V., IVIC, L. & KRIEGSTEIN, A. R. 2004. Cortical neurons arise in symmetric and asymmetric division zones and migrate through specific phases. *Nat Neurosci,* 7, 136-44.

O'DELL, R. S., USTINE, C. J., CAMERON, D. A., LAWLESS, S. M., WILLIAMS, R. M., ZIPFEL, W. R. & OLSON, E. C. 2012. Layer 6 cortical neurons require Reelin-Dab1 signaling for cellular orientation, Golgi deployment, and directed neurite growth into the marginal zone. *Neural Dev,* 7, 25.

PACARY, E., AZZARELLI, R. & GUILLEMOT, F. 2013. Rnd3 coordinates early steps of cortical neurogenesis through actin-dependent and -independent mechanisms. *Nat Commun,* 4, 1635.

PACARY, E., HENG, J., AZZARELLI, R., RIOU, P., CASTRO, D., LEBEL-POTTER, M., PARRAS, C., BELL, D. M., RIDLEY, A. J., PARSONS, M. & GUILLEMOT, F. 2011. Proneural transcription factors regulate different steps of cortical neuron migration through Rnd-mediated inhibition of RhoA signaling. *Neuron,* 69, 1069-84.

PHAN, K. D., HAZEN, V. M., FRENDO, M., JIA, Z. & BUTLER, S. J. 2010. The bone morphogenetic protein roof plate chemorepellent regulates the rate of commissural axonal growth. *J Neurosci,* 30, 15430-40.

PODKOWA, M., CHRISTOVA, T., ZHAO, X., JIAN, Y. & ATTISANO, L. 2013. p21-Activated kinase (PAK) is required for Bone Morphogenetic Protein (BMP)-induced dendritogenesis in cortical neurons. *Mol Cell Neurosci,* 57, 83-92.

PRASHAR, P., YADAV, P. S., SAMARJEET, F. & BANDYOPADHYAY, A. 2014. Microarray meta-analysis identifies evolutionarily conserved BMP signaling targets in developing long bones. *Dev Biol,* 389, 192-207.

RABALLO, R., RHEE, J., LYN-COOK, R., LECKMAN, J. F., SCHWARTZ, M. L. & VACCARINO, F. M. 2000. Basic fibroblast growth factor (Fgf2) is necessary for cell proliferation and neurogenesis in the developing cerebral cortex. *J Neurosci,* 20, 5012-23.

RAKIC, P. 1974. Neurons in Rhesus Monkey Visual Cortex: Systematic Relation between Time of Origin and Eventual Disposition. *Science,* 183, 425-427.

SEGKLIA, A., SEUNTJENS, E., ELKOURIS, M., TSALAVOS, S., STAPPERS, E., MITSIADIS, T. A., HUYLEBROECK, D., REMBOUTSIKA, E. & GRAF, D. 2012. Bmp7 regulates the survival, proliferation, and neurogenic properties of neural progenitor cells during corticogenesis in the mouse. *PLoS One,* 7, e34088.

SHIMOGORI, T., BANUCHI, V., NG, H. Y., STRAUSS, J. B. & GROVE, E. A. 2004. Embryonic signaling centers expressing BMP, WNT and FGF proteins interact to pattern the cerebral cortex. *Development,* 131, 5639-47.

SIEGENTHALER, J. A., ASHIQUE, A. M., ZARBALIS, K., PATTERSON, K. P., HECHT, J. H., KANE, M. A., FOLIAS, A. E., CHOE, Y., MAY, S. R., KUME, T., NAPOLI, J. L., PETERSON, A. S. & PLEASURE, S. J. 2009. Retinoic acid from the meninges regulates cortical neuron generation. *Cell,* 139, 597-609.

TABATA, H. & NAKAJIMA, K. 2003. Multipolar migration: the third mode of radial neuronal migration in the developing cerebral cortex. *J Neurosci,* 23, 9996-10001.

WOODHEAD, G. J., MUTCH, C. A., OLSON, E. C. & CHENN, A. 2006. Cell-autonomous beta-catenin signaling regulates cortical precursor proliferation. *J Neurosci,* 26, 12620-30.

ZHANG, D., MEHLER, M. F., SONG, Q. & KESSLER, J. A. 1998. Development of bone morphogenetic protein receptors in the nervous system and possible roles in regulating trkC expression. *J Neurosci,* 18, 3314-26.

ZHU, H., KAVSAK, P., ABDOLLAH, S., WRANA, J. L. & THOMSEN, G. H. 1999. A SMAD ubiquitin ligase targets the BMP pathway and affects embryonic pattern formation. *Nature,* 400, 687-93.

Figures

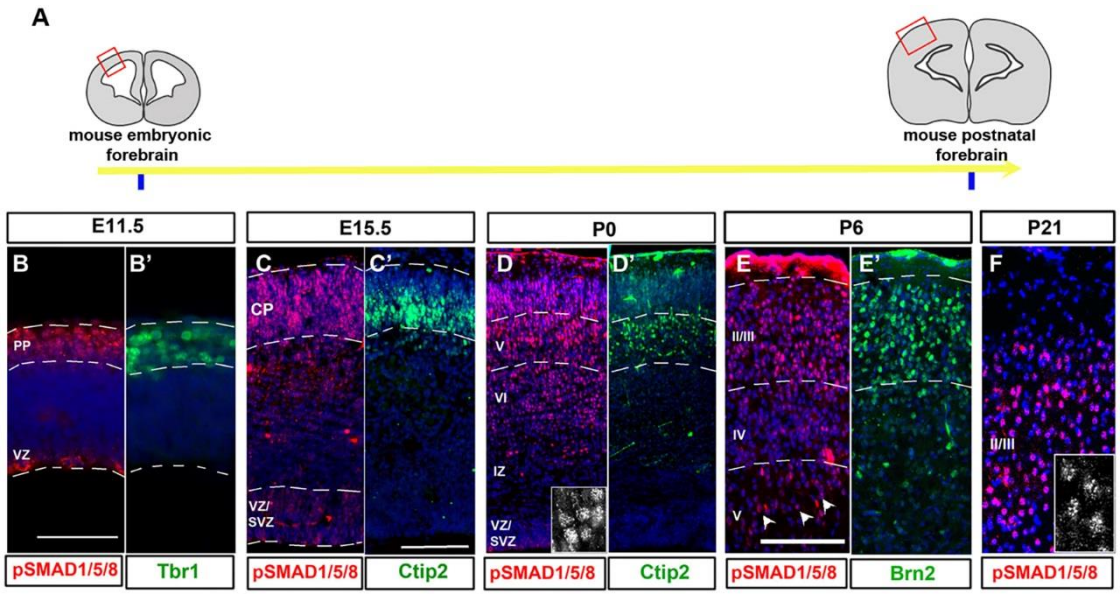

Figure 1. Detection of BMP signaling in the mouse cortex at different developmental time points. (A) Schematic of mouse forebrain section at E11.5 and at Postnatal Day 21(P21). (B-F) Immunohistochemical detection of pSMAD1/5/8 in the mouse cortex at E11.5 (B), E15.5 (C), P0 (D), P6 (E) and P21 (F). (B'-E') Immunohistochemical detection of layer specific markers Tbr1 (B'), Ctip2 (C' and D') and Brn2 (E'). Scale bar: 200µm (B and B') and 100 µm (C-E and C'-E').

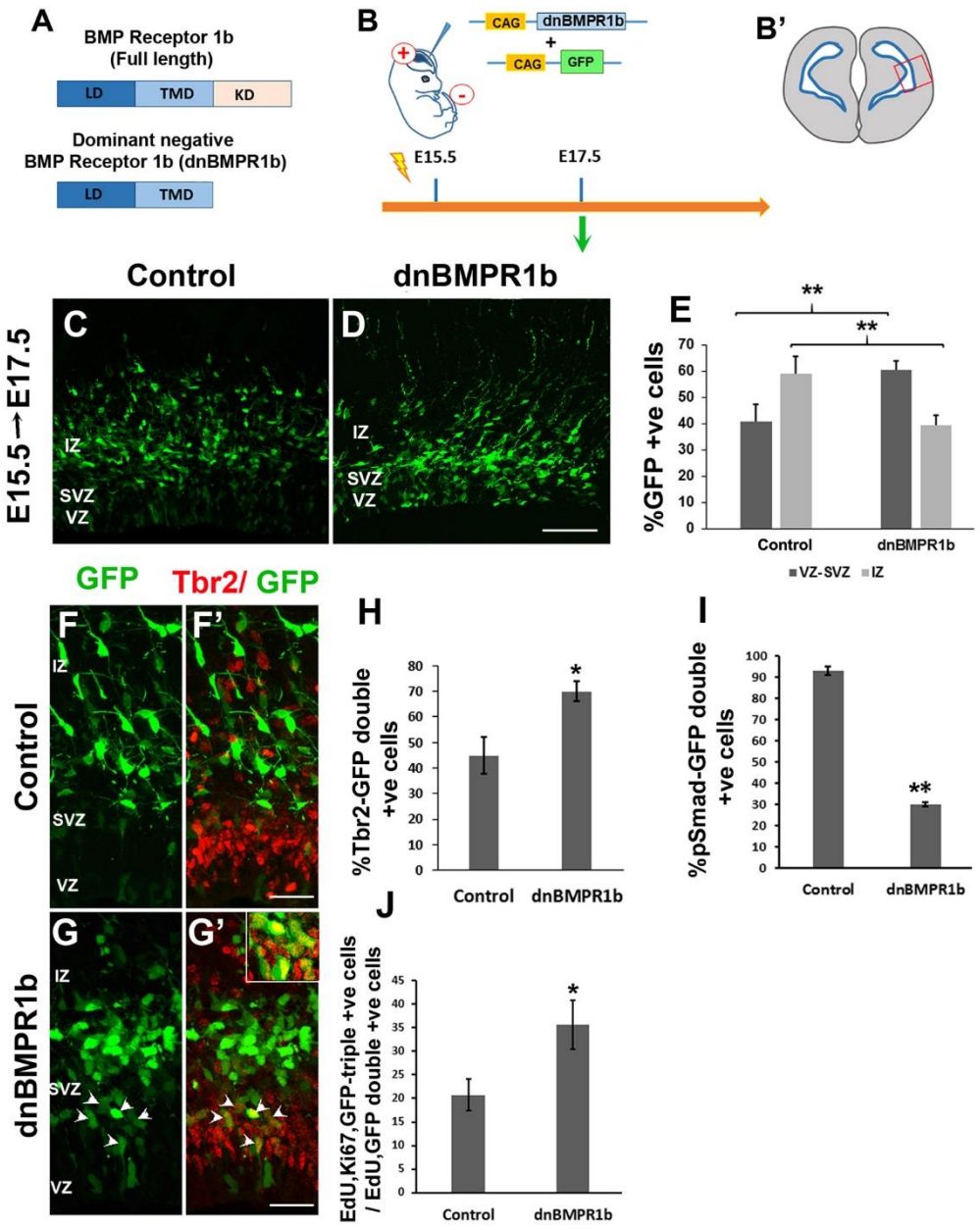

Figure 2. Early effects of overexpression of dnBMPR1b on migration of E15.5 born upper layer neurons. (A) Schematic showing full length BMP receptor 1b and its dominant negative version (LD = ligand binding domain, TMD = trans-membrane domain and KD = Kinase domain). (B) Experimental strategy used. (B') Schematic of cortical section with boxed region corresponding to images C-D. (C-D) Images of the mouse cortex overexpressing GFP (C) and dnBMPR1b (D) 48 hours after electroporation at E15.5. (E) Quantification of distribution of GFP-positive cells 48 hours after electroporation. (F-H) Co-immunostaining for Tbr2 and GFP in the cortical sections 48 hours after electroporation in control (F') and test animals (G' and

inset) and its quantification (H). (I) Quantification of pSMAD1/5/8-GFP double positive cells in test and control animals. (J) Quantification showing GFP-EdU-Ki67 triple positive cells among GFP-EdU double positive cells for test and control animals. Quantification data is represented as % Mean ± STD (n=3), *$p<0.05$ and **$p<0.005$. Scale bar: 100µm (C and D) and 50 µm (F-G).

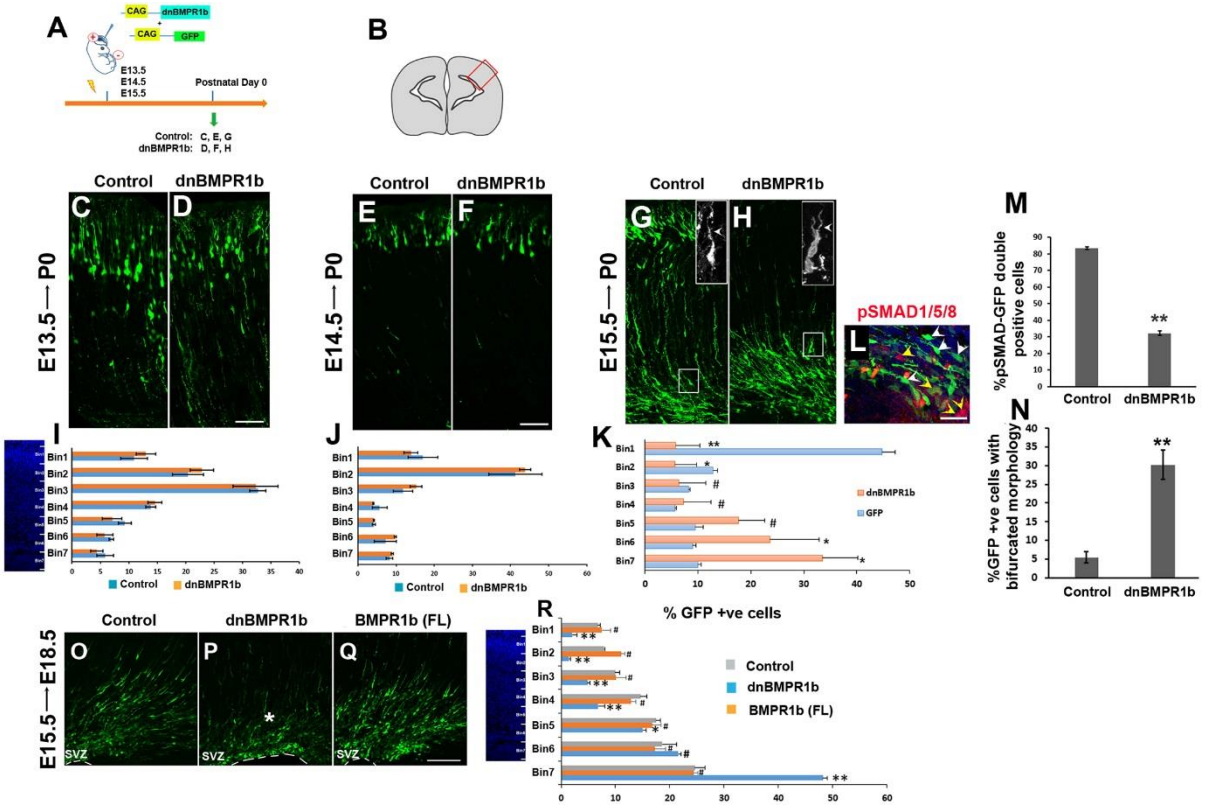

Figure 3. Effect of inhibition of BMP signaling on migration of cortical neurons born at E13.5, E14.5 and E15.5.

(A) Experimental strategy used, (B) The red box in the schematic of the cortical section corresponds to panels C -H. (C-H) Images of mouse cortex electroporated with pCAG-GFP at E13.5 (C), E14.5 (E) and E15.5 (G) and electroporated with pCAG-dnBMPR1b at E13.5 (D), E14.5 (F) and E15.5 (H). (G and H, insets) The morphology of leading process in the control and test animals (white arrowheads). (I-K) Quantification of GFP positive cells present in each bin in the cortex at P0 in animals electroporated at E13.5 (I), E14.5 (J) and at E15.5 (K). (L) Immunostaining for pSMAD1/5/8 in the cortical section of test animals at P0 showing pSMAD1/5/8-negative (white arrowheads), and pSMAD1/5/8-positive cells (yellow arrowheads) among the GFP-positive cells and its quantification (M). (N) Quantification of the cells with bifurcated leading process in test and control animals. *n=3*; **p<0.005, *p<0.05 and #p>0.05. Scale bar: 100µm (C, D and M).

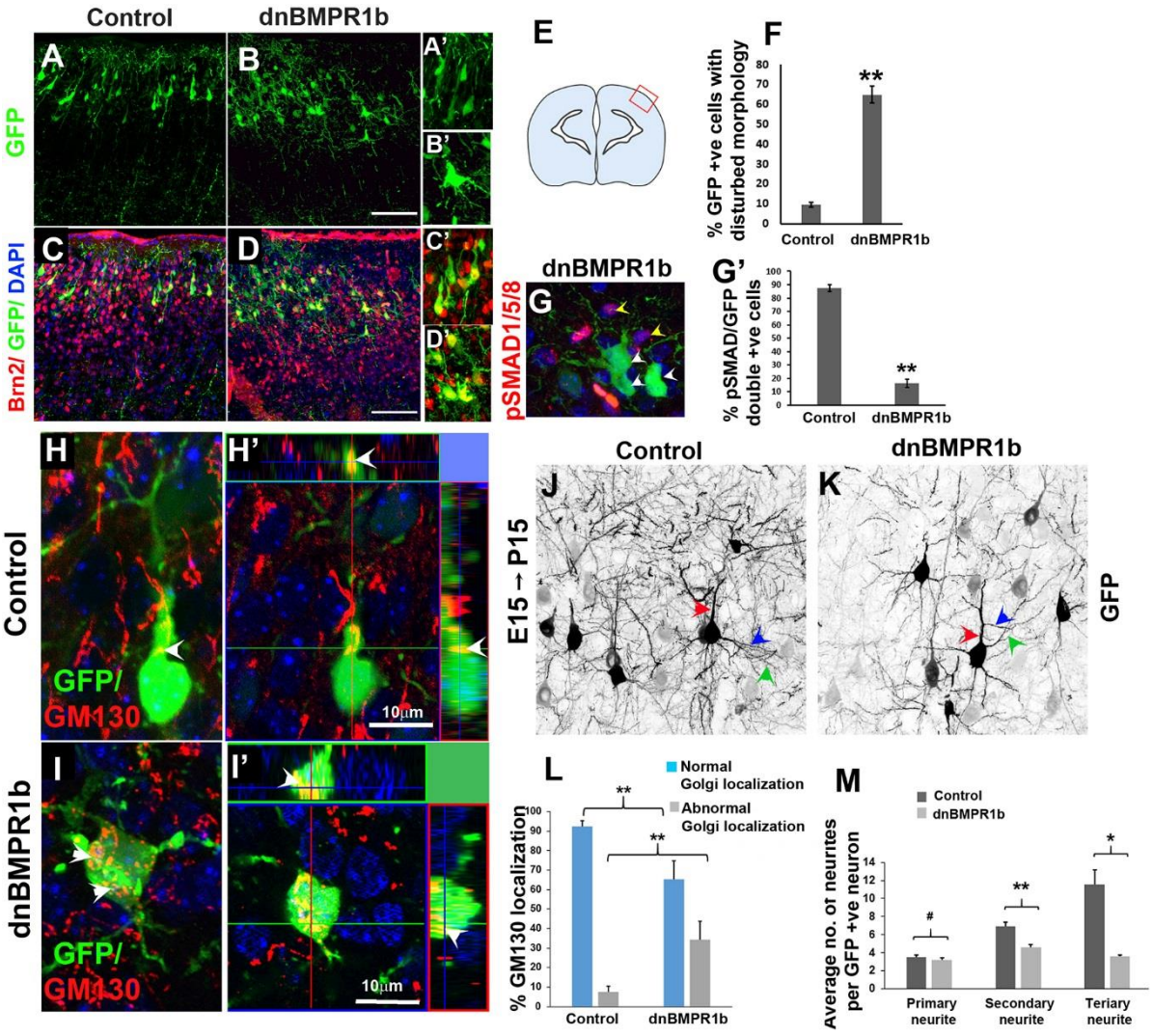

Figure 4. Effect of overexpression of dnBMPR1b on polarity and dendritic branching of E15.5 born upper layer cortical neurons.

(A-D) Images from the boxed region shown in the schematic (E) showing GFP-positive cells present in Brn2 positive domain in the mouse cortex overexpressing GFP (A and C), and dnBMPR1b (B and D) at P6. (A'-D') High magnification images from image A - D, showing morphology of GFP positive cells in control (A') and expression of Brn2 (C') and the disturbed morphology of GFP positive cells in test animal (B') and expression of Brn2 (D'). (F) Quantification of GFP positive cells with disturbed morphology in test and control animals at P6. (G and G') Image from the cortical section of test animals showing pSMAD1/5/8-negative GFP positive cells (white arrowheads) among pSMAD1/5/8 positive cells (yellow arrowheads)

and its quantification (G'). (H-I) Images of the cortex of control (H) and test (I) at P6, showing localization of GM130 (white arrowheads)). (H'-I') the orthogonal projection images corresponding to H and I. (L) Quantification of GFP positive cells with normal and abnormal Golgi localization in control and test animals (n=4). (J and K) Colour-inverted images of GFP positive cells in the mouse cortex at P15 showing primary (red arrowhead), secondary (blue arrowhead) and tertiary neurites (green arrowhead) in control (J) and test animals (K). (M) Quantification of the number of primary, secondary and tertiary neurites per GFP positive cell (n=4 and ~50 cells per n). Quantification data is represented as % Mean ±STD, *p<0.05, **p<0.005 and #p>0.05. Scale bar: 100 µm (A -D), and 10µm (H and I).

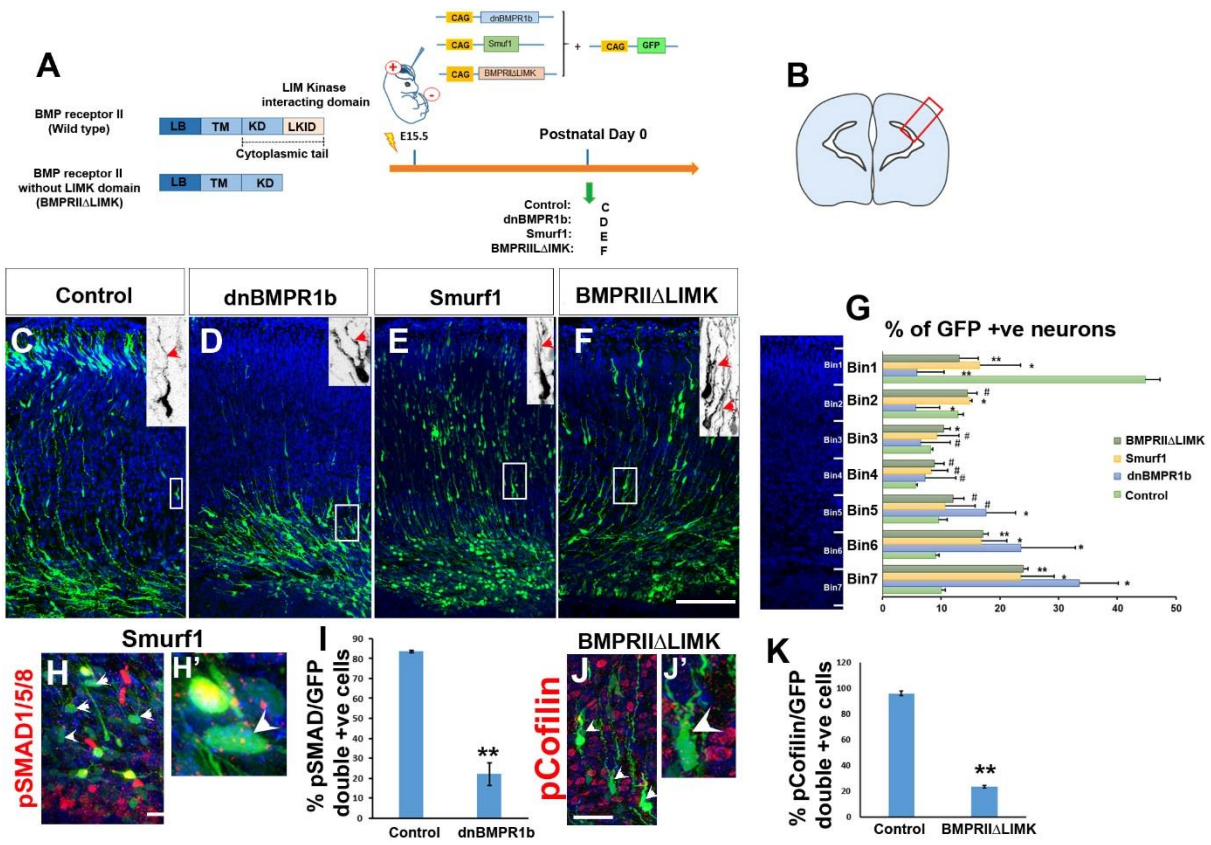

Figure 5. Effect of inhibition of canonical and non-canonical BMP signaling on migration of E15.5 born upper layer cortical neurons.

(A) Diagrammatic representation of full length BMPRII and BMPRII lacking LIMK interacting domain (LB: ligand binding domain, TM: trans-membrane domain, KD: kinase domain and LKID: LIMK interacting domain) and the experimental strategy used. (B) The boxed region in the cortical section schematic corresponds to images C-F. (C-F) Images of the mouse cortex at P0 overexpressing GFP (C), dnBMPR1b (D), Smurf1 (E) and BMPRIIΔLIMK (F). (C-F, insets) Color-inverted images showing the leading process (red arrowheads) of migrating neurons from the boxed region in the images C-F. (G) Quantification of the distribution of GFP positive cells across the cortex upon overexpression of the above-mentioned constructs. (H, H') Immunostaining showing pSMAD1/5/8 negative GFP positive cells in Smurf1 overexpressing cortex (white arrowheads) and its quantification (I). (J, J') Immunostaining showing p-Cofilin-negative GFP positive cells in the BMPRIIΔLIMK

electroporated cortex (white arrowheads) and its quantification (K). Data is represented as % Mean ±STD, (n=3), *p<0.05, **p<0.005 and #p>0.05. Scale bar: 100µm (C-F) and 50µm (H and J).

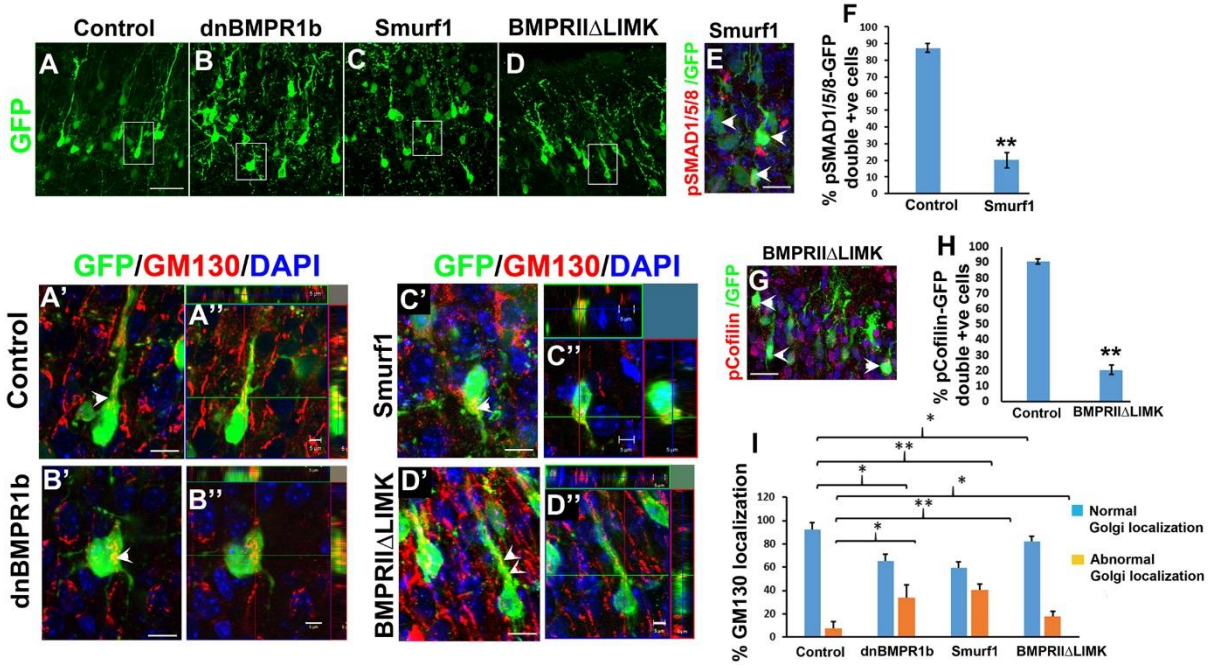

Figure 6. Effect of inhibition of canonical and non-canonical BMP signaling on polarity and dendritic branch formation in E15.5 born upper layer cortical neurons.

(A-D) Images from the cortex overexpressing GFP (A), dnBMPR1b (B), Smurf1 (C) and BMPRIIΔLIMK (D) showing neuronal morphology at P6.(A'-D') Magnified images of GFP positive neurons corresponding to the boxed region in A-D, showing GM130 localisation for control (A', white arrowhead), dnBMPR1b (B' white arrowhead), Smurf1 (C', white arrowhead) and BMPRIIΔLIMK (D', white arrowhead) and its quantification (I; *n*=3, ~50 cells per *n*). (A''-D'') The orthogonal projection images corresponding to A'-D'. (E) Immunostaining showing pSMAD1/5/8 negative GFP positive cells (white arrowhead) in Smurf1 overexpressing cortex s and its quantification (F). (G) Immunostaining showing p-Cofilin-negative GFP positive cells (white arrowheads) in the BMPRIIΔLIMK electroporated cortex and its quantification (H). Quantification data is represented as % Mean ±STD. (*n*=3 and ~20 cells per n)). *p<0.05, **p<0.005 and #p>0.05. Scale bar: 50 µm (A-D and A'-D') and 20 µm (E and G).

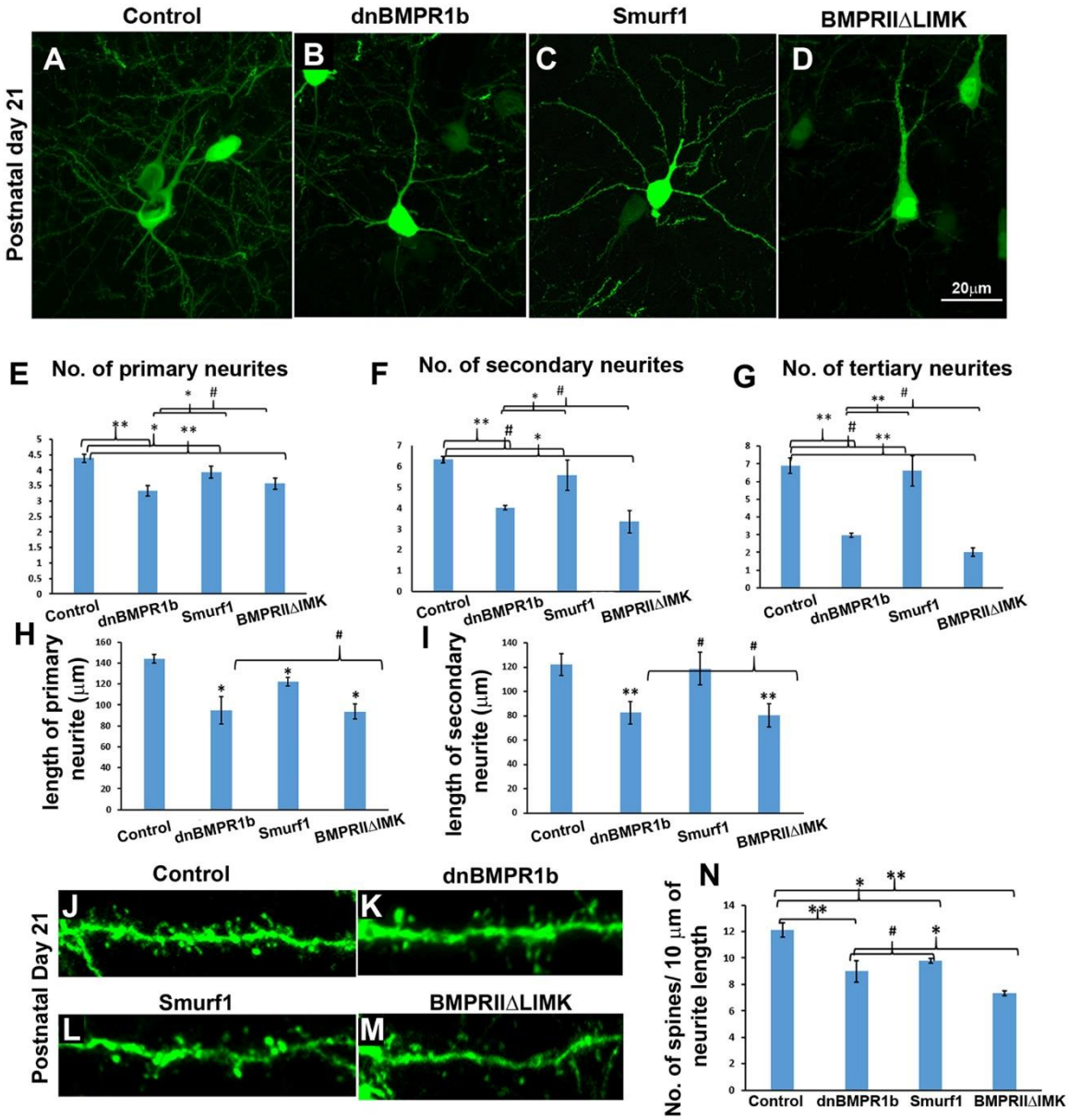

Figure 7. The effect of canonical and non-canonical BMP signaling on dendritogenesis, of E15.5 born upper layer cortical neurons.

(A-D) Images of the neurons overexpressing GFP (A), dnBMPR1b (B), Smurf1 (C) and BMPRIIΔLIMK (D). (E-I) Quantification of number of primary (E), secondary (F), tertiary (G) neurites and quantification of neurite length of primary (H) and secondary (I) neurites in neurons overexpressing GFP, dnBMPR1b, Smurf1 and BMPRIIΔLIMK. (J-M) Magnified image of dendrites of neurons overexpressing GFP (J), dnBMPR1b (K), Smurf1 (L) and BMPRIIΔLIMK (M) showing dendritic spines and the quantification of spine density (N).

Quantification data is represented as % Mean ±STD. (*n*=3 and ~20 cells per n)). *p<0.05, **p<0.005 and #p>0.05.

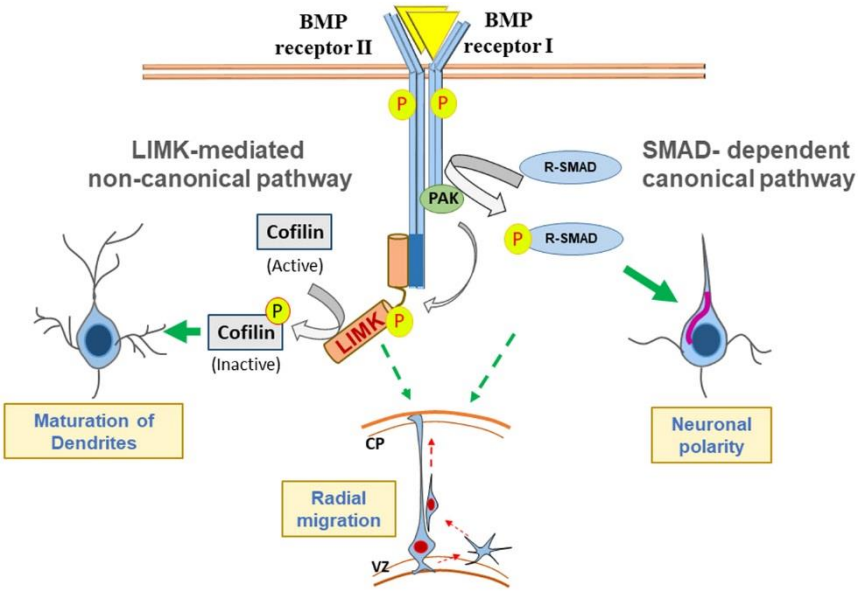

Figure 8. Schematic depiction of SMAD-dependent canonical and LIMK-mediated non-canonical BMP pathways and their possible involvement in multiple aspects of mouse cortex development.

Radial migration of upper layer cortical neurons is regulated by both of these pathways whereas the establishment of neuronal polarity is mostly through the SMAD-dependent canonical BMP signalling pathway. On the other hand, dendritic maturation of cortical neurons is regulated by LIMK-mediated non-canonical BMP pathway.

Experimental Procedure:

Cloning of constructs:

(1) pCAG-dnBMPR1b: chicken dnBMPR1b originally cloned into an avian retroviral backbone (RCAS-dnBMPR1b) (Kawakami et al., 1996) and obtained as a gift from Prof. Clifford J. Tabin, Harvard Medical School, Boston, USA, was sub-cloned at ClaI sites into a modified pCAG backbone (Gupta and Sen, 2015). (4) pCAG-BMPRIIΔLIMK: human BMPRIIΔLIMK from pCDNA-BMPRIIΔLIMK (gift from Prof. Samantha Butler, University of California Los Angeles, LA, USA) (Phan et al., 2010) was further sub-cloned into the modified pCAG backbone (Gupta and Sen, 2015) between ECoRI and NotI sites . (3) pCAG-Smurf1: mouse Smurf1 cDNA originally cloned into pCMV-SPORT6 (Gene bank accession no. BC029097, Mouse full length cDNA clone library) was further sub-cloned into modified pCAG backbone (Gupta and Sen, 2015) at ECoRV sites. (4). pCAG-mCherry: mCherry cDNA was subcloned in to modified pCAG backbone between ECoRI- NotI sites.

Immunohistochemistry:

Mouse forebrain sections at different developmental stages were post-fixed in 4% paraformaldehyde (PFA) in PBS, permeabilized with PBT (0.2% triton in 1xPBS) followed by blocking in 5% goat serum at room temperature for 1 hour. Sections were further incubated with the primary antibodies overnight at 4^0C followed by incubation with their respective secondary antibody at room temperature. Fluorescence signal was developed by using following secondary antibodies: anti-mouse (Cat.no. 111-585-003, Jackson ImmunoResearch Laboratories Inc.), anti-rabbit (Cat. No. 111-545-003, Jackson ImmunoResearch Laboratories Inc.), anti-goat (Cat.no. 705-165-003, Jackson ImmunoResearch Laboratories Inc.) and anti-chicken (Cat.no.103-165-155, Jackson ImmunoResearch Laboratories Inc.).

Quantification:

For quantification, each electroporated embryo analysed was considered as a biological replicate (n) and for each biological replicate, three to five consecutive brain sections were analysed which was considered as technical replicates (N). GFP positive cells from all of the technical replicate corresponding to each biological replicate (n) were counted and the mean was calculated. For cell polarity analysis, the GFP positive neuron with the Golgi localization through the apical dendrite was considered as normal cell while the cell with random Golgi localization within the cell body was considered as abnormal cell. For quantification of dendritic branches, the mean number of primary, secondary and tertiary branches were calculated for ~ 50 GFP positive neurons per animal (n = 3). The mean and standard deviation plotted on the graph were calculated from the mean of all the biological replicates. Quantification data is represented as % Mean ± Standard deviation.

Cell-based assay for testing efficacy of constructs used:

293T cells were used for a cell-based assay to test the efficacy of the constructs used. Cells plated in a 24-well plate were transfected with 1µg DNA corresponding to the following constructs: 1) pCAG-dnBMPR1b + pCAG-GFP, 2) pCAG-BMPRIIΔLIMK+ pCAG-GFP and 3) pCAG-Smurf1+ pCAG-GFP using TurboFect transfection reagent (Cat no. R0531, Thermo Fisher Scientific). The control set of cells were transfected with pCAG-GFP alone. After 24 hours of transfection, immunocytochemistry was performed for detection of pSmad1/5/8 and p-Cofilin in each set of cells as described previously. For each construct, the transfection was done in triplicates (n=3) and nearly 300 cells were counted from each replicate to quantify the percentage of GFP positive cells that were either pSmad1/5/8 positive and/or p-Cofilin positive. Quantification data is represented as % Mean ± Standard deviation.

Figure S1.

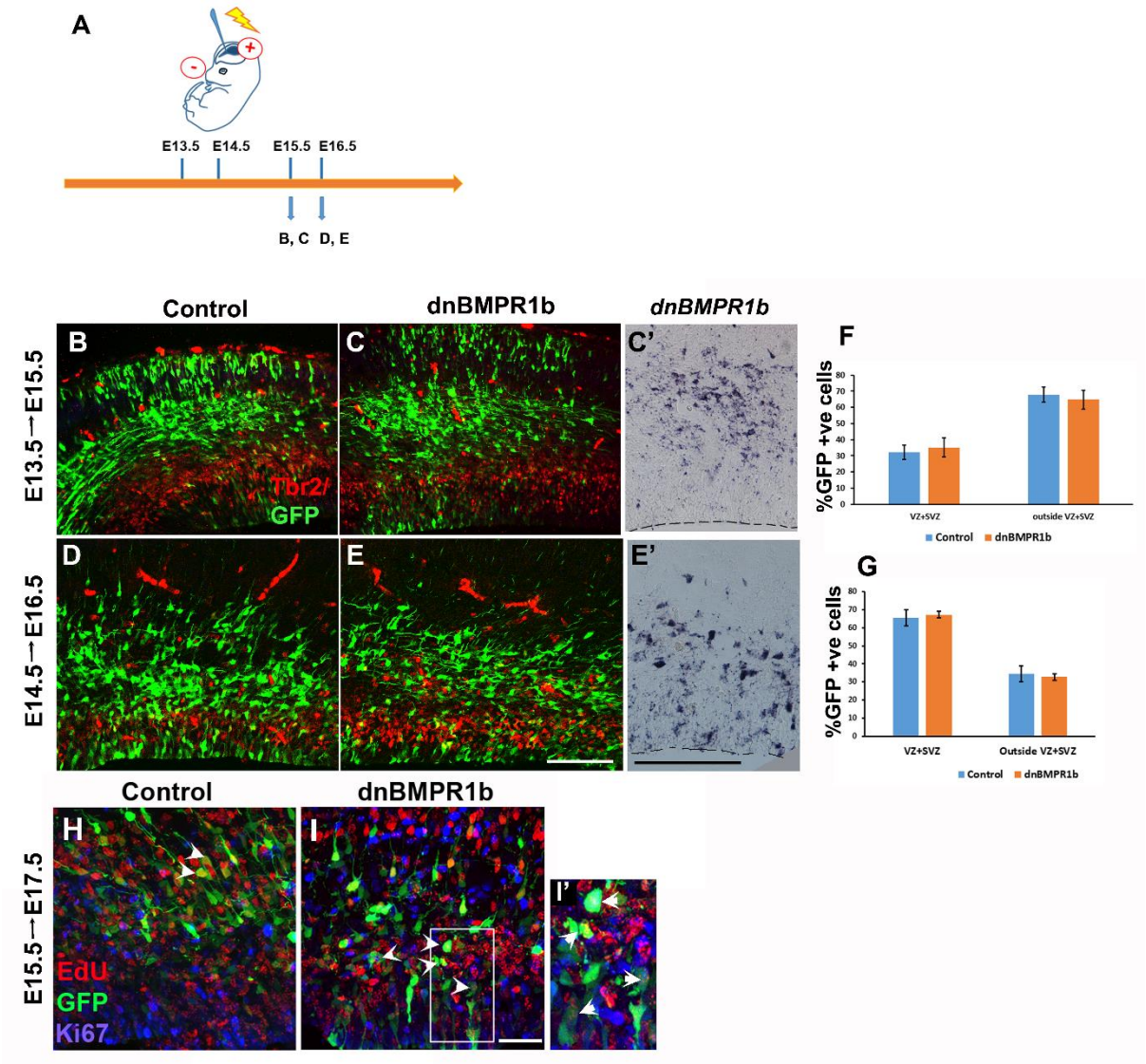

Figure S1: (A) Schematic for experimental design. (B-E) Immunohistochemistry for Tbr2 in the cortex electroporated with pCAG-GFP and pCAG-dnBMPR1b at E13.5 analysed at E15.5 (B and C) and electroporated at E14.5 and analysed at E16.5 (D and E). (C' and E') mRNA in situ hybridization for detecting the transcript of dnBMPR1b in the cortical sections 48 hours after electroporation performed at E13.5 (C') and E14.5 (E'). (F and G) Quantification of GFP positive cells in the VZ-SVZ and outside the VZ-SVZ demarcated by Tbr2 expression domain in the cortex electroporated at E13.5 (F) and E14.5 (G). (H, I and I') Images of the cortices

electroporated with pCAG-GFP (H) and pCAG-dnBMPR1b (I, I') showing Ki67, GFP and EDU triple positive cells (white arrowheads). Quantification data is represented as % Mean ± STD (n=3), *p<0.05 and **p<0.005. Scale bar: 100µm (B-E) and 50 µm (H and I).

Figure S2.

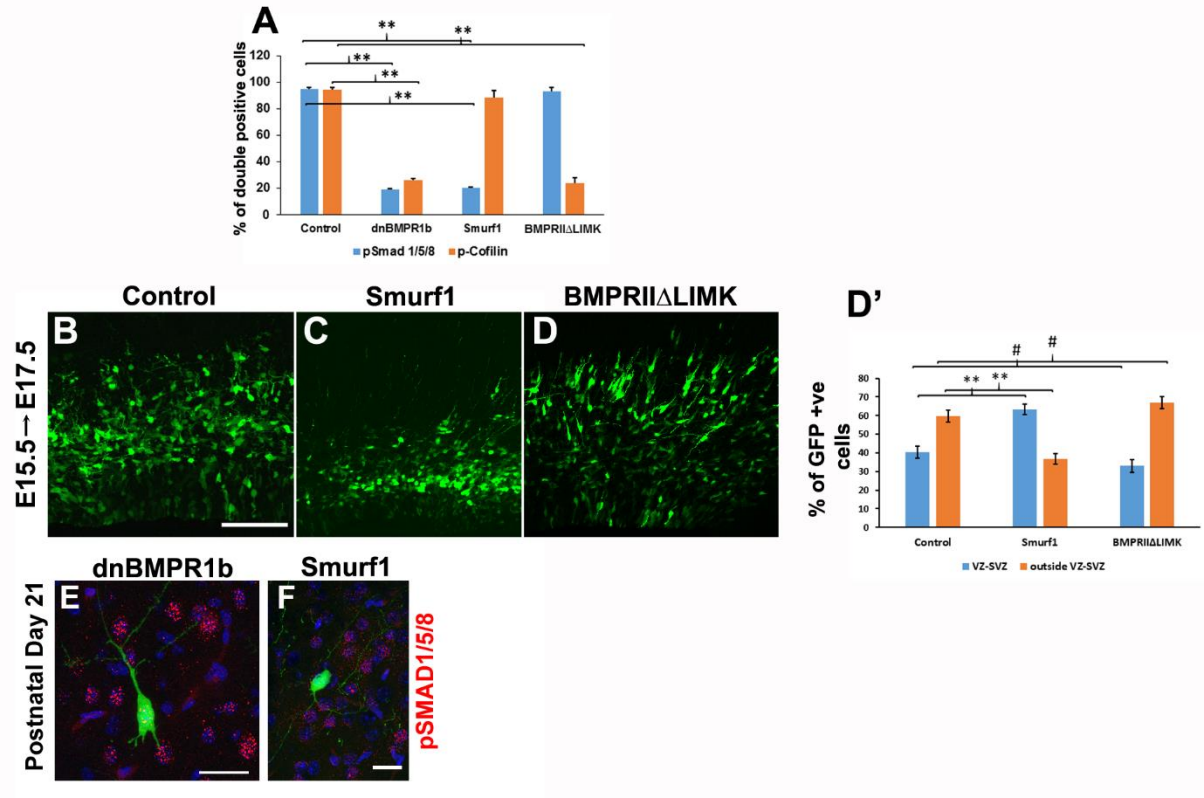

Figure S2: (A) Quantification showing GFP-pSMAD1/5/8 and GFP-p-Cofilin double positive cells transfected with pCAG-GFP (Control), pCAG-dnBMPR1b, pCAG-Smurf1 and pCAG-BMPRIIΔLIMK along with pCAG-GFP. Quantification data is represented as % mean ± STD. **p<0.005. (B-D) Image of the cortex overexpressing GFP (B), Smurf1 (C) and

BMPRIIΔLIMK (D) showing the distribution of GFP positive cells in the VZ-SVZ and the IZ in the cortex at E17.5. (D') Quantification of the distribution of GFP positive cells in the cortex expressing GFP, Smurf1 and BMPRIIΔLIMK at E17.5. (E and F) immunostaining showing pSMAD1/5/8 in the cortex overexpressing dnBMPR1b (E) and Smurf1 (F) at P21. Scale bar: 100 µm (B-D) and 20 µm (E-F).

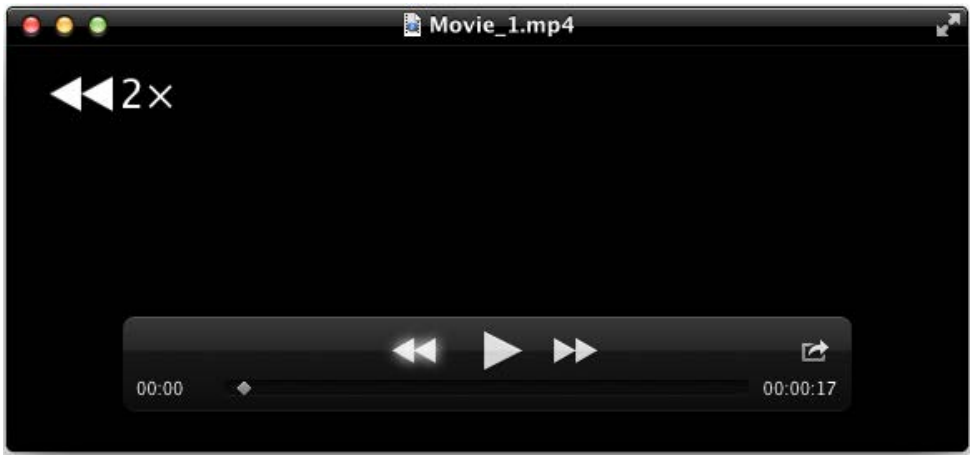

Movie 1

A multi-angle rotational view of GFP positive cell from the control cortex at P6 showing the Golgi localization within the GFP positive domain.

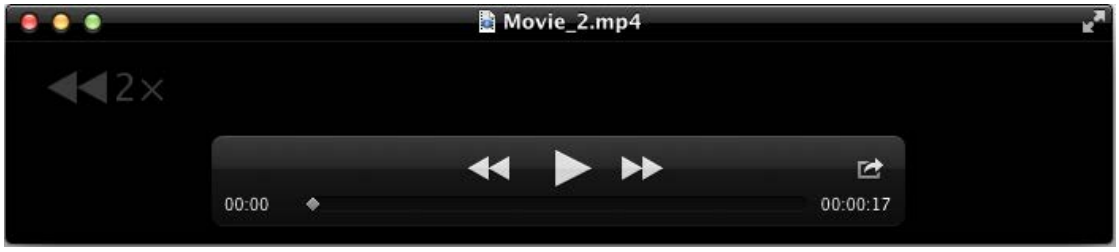

Movie 2

A multi-angle rotational view of GFP positive cell from the dnBMPR1b electroporated cortex at P6 showing random Golgi localization in the cell body.

References:

GUPTA, S. & SEN, J. 2015. Retinoic acid signaling regulates development of the dorsal forebrain midline and the choroid plexus in the chick. *Development,* 142**,** 1293-8.

KAWAKAMI, Y., ISHIKAWA, T., SHIMABARA, M., TANDA, N., ENOMOTO-IWAMOTO, M., IWAMOTO, M., KUWANA, T., UEKI, A., NOJI, S. & NOHNO, T. 1996. BMP signaling during bone pattern determination in the developing limb. *Development,* 122**,** 3557-66.

PHAN, K. D., HAZEN, V. M., FRENDO, M., JIA, Z. & BUTLER, S. J. 2010. The bone morphogenetic protein roof plate chemorepellent regulates the rate of commissural axonal growth. *J Neurosci,* 30**,** 15430-40.

Experimental Procedure:

Cloning of constructs:

(1) pCAG-dnBMPR1b: chicken dnBMPR1b originally cloned into an avian retroviral backbone (RCAS-dnBMPR1b) (Kawakami et al., 1996) and obtained as a gift from Prof. Clifford J. Tabin, Harvard Medical School, Boston, USA, was sub-cloned at ClaI sites into a modified pCAG backbone (Gupta and Sen, 2015). (4) pCAG-BMPRIIΔLIMK: human BMPRIIΔLIMK from pCDNA-BMPRIIΔLIMK (gift from Prof. Samantha Butler, University of California Los Angeles, LA, USA) (Phan et al., 2010) was further sub-cloned into the modified pCAG backbone (Gupta and Sen, 2015) between ECoRI and NotI sites . (3) pCAG-Smurf1: mouse Smurf1 cDNA originally cloned into pCMV-SPORT6 (Gene bank accession no. BC029097, Mouse full length cDNA clone library) was further sub-cloned into modified pCAG backbone (Gupta and Sen, 2015) at ECoRV sites. (4). pCAG-mCherry: mCherry cDNA was subcloned in to modified pCAG backbone between ECoRI- NotI sites.

Immunohistochemistry:

Mouse forebrain sections at different developmental stages were post-fixed in 4% paraformaldehyde (PFA) in PBS, permeabilized with PBT (0.2% triton in 1xPBS) followed by blocking in 5% goat serum at room temperature for 1 hour. Sections were further incubated with the primary antibodies overnight at 4^0C followed by incubation with their respective secondary antibody at room temperature. Fluorescence signal was developed by using following secondary antibodies: anti-mouse (Cat.no. 111-585-003, Jackson ImmunoResearch Laboratories Inc.), anti-rabbit (Cat. No. 111-545-003, Jackson ImmunoResearch Laboratories Inc.), anti-goat (Cat.no. 705-165-003, Jackson ImmunoResearch Laboratories Inc.) and anti-chicken (Cat.no.103-165-155, Jackson ImmunoResearch Laboratories Inc.).

Quantification:

For quantification, each electroporated embryo analysed was considered as a biological replicate (n) and for each biological replicate, three to five consecutive brain sections were analysed which was considered as technical replicates (N). GFP positive cells from all of the technical replicate corresponding to each biological replicate (n) were counted and the mean was calculated. For cell polarity analysis, the GFP positive neuron with the Golgi localization through the apical dendrite was considered as normal cell while the cell with random Golgi localization within the cell body was considered as abnormal cell. For quantification of dendritic branches, the mean number of primary, secondary and tertiary branches were calculated for ~ 50 GFP positive neurons per animal (n = 3). The mean and standard deviation plotted on the graph were calculated from the mean of all the biological replicates. Quantification data is represented as % Mean ± Standard deviation.

Cell-based assay for testing efficacy of constructs used:

293T cells were used for a cell-based assay to test the efficacy of the constructs used. Cells plated in a 24-well plate were transfected with 1µg DNA corresponding to the following constructs: 1) pCAG-dnBMPR1b + pCAG-GFP, 2) pCAG-BMPRIIΔLIMK+ pCAG-GFP and 3) pCAG-Smurf1+ pCAG-GFP using TurboFect transfection reagent (Cat no. R0531, Thermo Fisher Scientific). The control set of cells were transfected with pCAG-GFP alone. After 24 hours of transfection, immunocytochemistry was performed for detection of pSmad1/5/8 and p-Cofilin in each set of cells as described previously. For each construct, the transfection was done in triplicates (n=3) and nearly 300 cells were counted from each replicate to quantify the percentage of GFP positive cells that were either pSmad1/5/8 positive and/or p-Cofilin positive. Quantification data is represented as % Mean ± Standard deviation.

Figure S1.

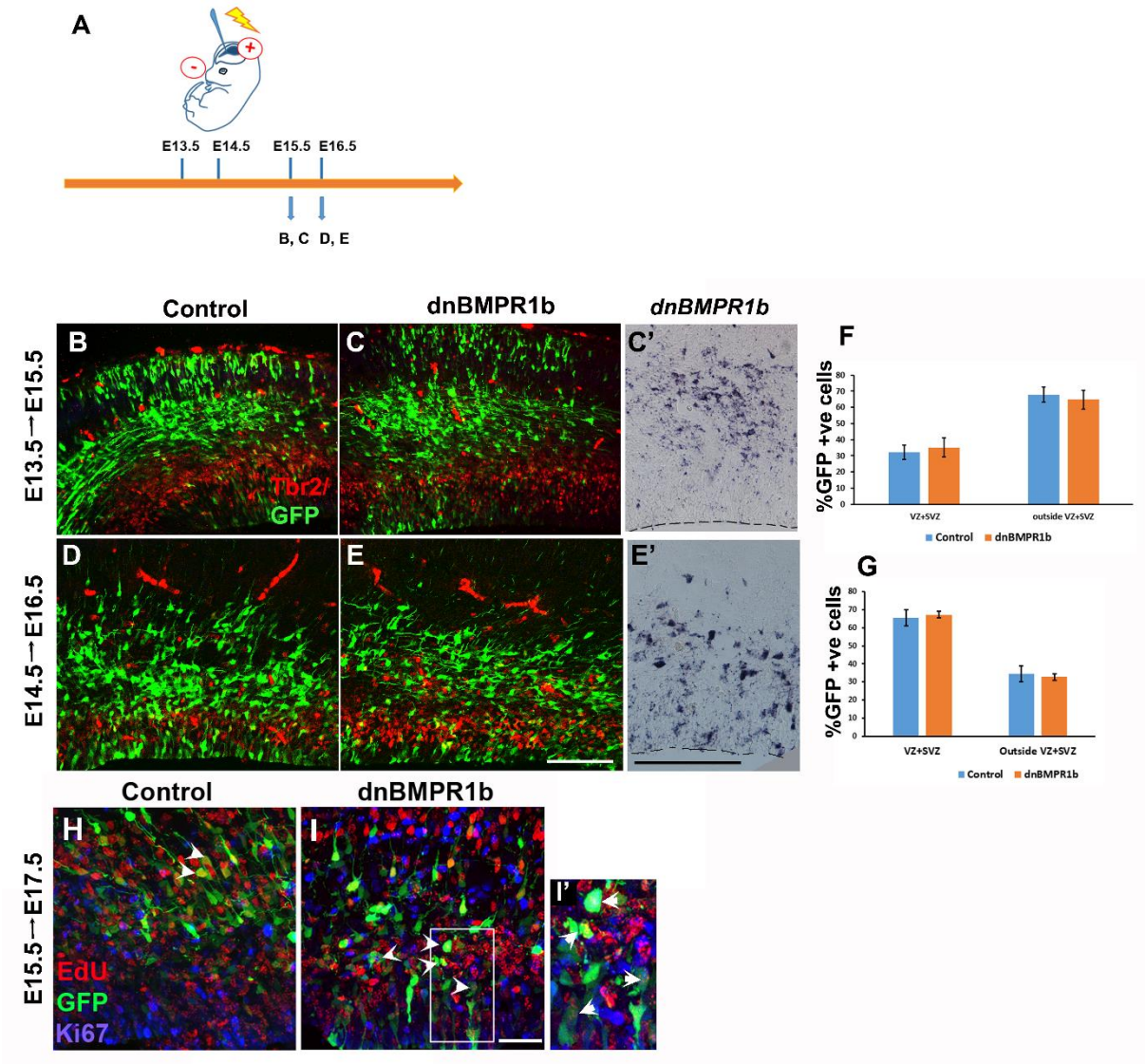

Figure S1: (A) Schematic for experimental design. (B-E) Immunohistochemistry for Tbr2 in the cortex electroporated with pCAG-GFP and pCAG-dnBMPR1b at E13.5 analysed at E15.5 (B and C) and electroporated at E14.5 and analysed at E16.5 (D and E). (C' and E') mRNA in situ hybridization for detecting the transcript of dnBMPR1b in the cortical sections 48 hours after electroporation performed at E13.5 (C') and E14.5 (E'). (F and G) Quantification of GFP positive cells in the VZ-SVZ and outside the VZ-SVZ demarcated by Tbr2 expression domain in the cortex electroporated at E13.5 (F) and E14.5 (G). (H, I and I') Images of the cortices

electroporated with pCAG-GFP (H) and pCAG-dnBMPR1b (I, I') showing Ki67, GFP and EDU triple positive cells (white arrowheads). Quantification data is represented as % Mean ± STD (n=3), *p<0.05 and **p<0.005. Scale bar: 100µm (B-E) and 50 µm (H and I).

Figure S2.

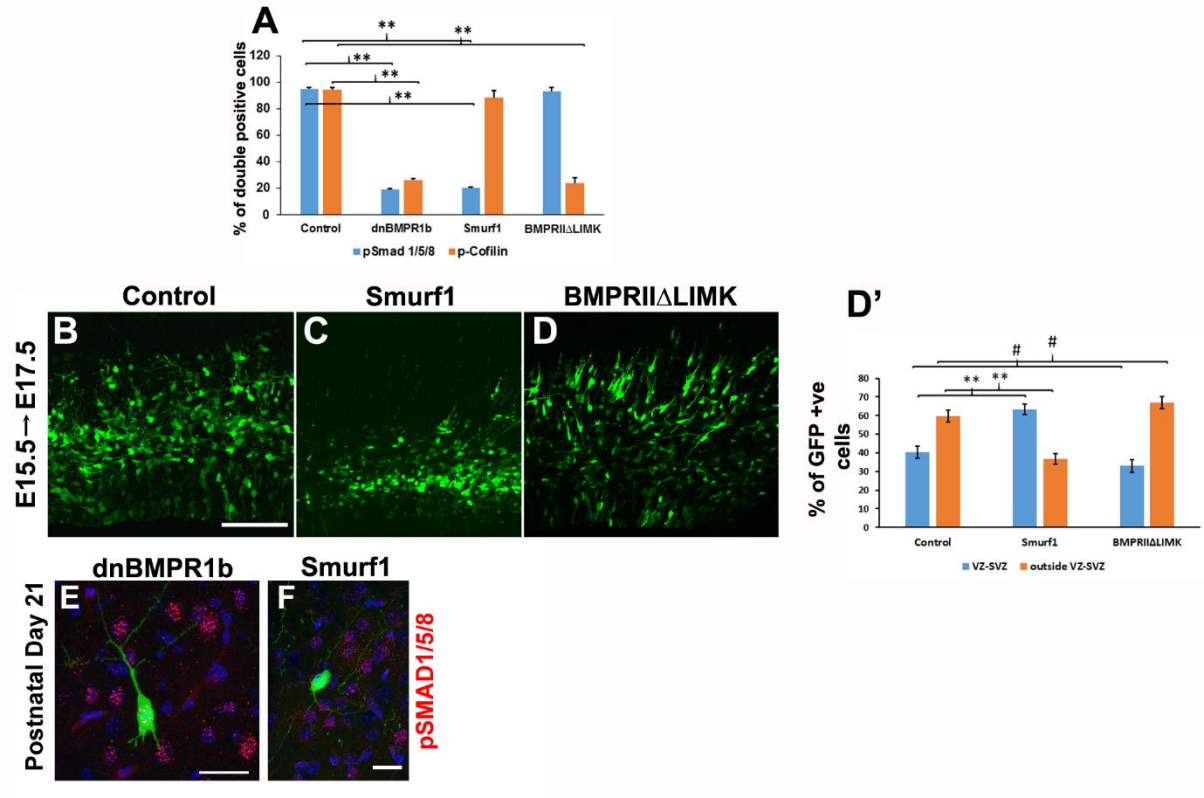

Figure S2: (A) Quantification showing GFP-pSMAD1/5/8 and GFP-p-Cofilin double positive cells transfected with pCAG-GFP (Control), pCAG-dnBMPR1b, pCAG-Smurf1 and pCAG-BMPRIIΔLIMK along with pCAG-GFP. Quantification data is represented as % mean ± STD. **p<0.005. (B-D) Image of the cortex overexpressing GFP (B), Smurf1 (C) and

BMPRIIΔLIMK (D) showing the distribution of GFP positive cells in the VZ-SVZ and the IZ in the cortex at E17.5. (D') Quantification of the distribution of GFP positive cells in the cortex expressing GFP, Smurf1 and BMPRIIΔLIMK at E17.5. (E and F) immunostaining showing pSMAD1/5/8 in the cortex overexpressing dnBMPR1b (E) and Smurf1 (F) at P21. Scale bar: 100 µm (B-D) and 20 µm (E-F).

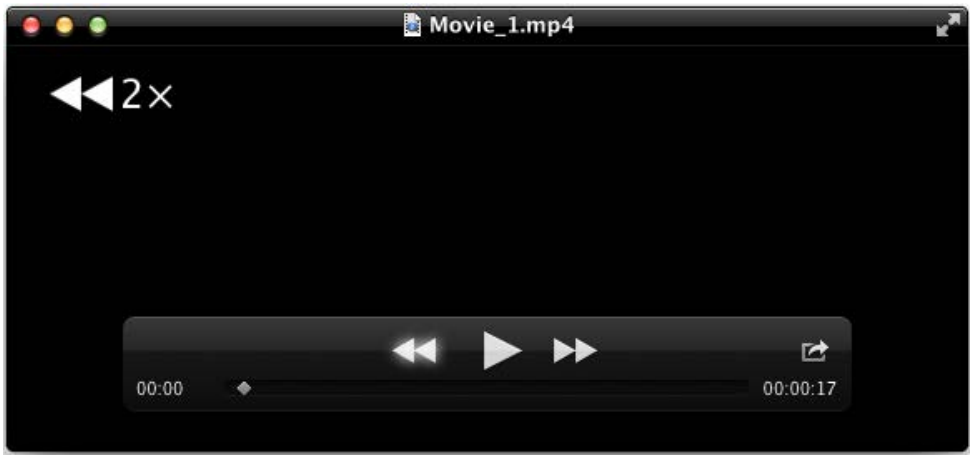

Movie 1

A multi-angle rotational view of GFP positive cell from the control cortex at P6 showing the Golgi localization within the GFP positive domain.

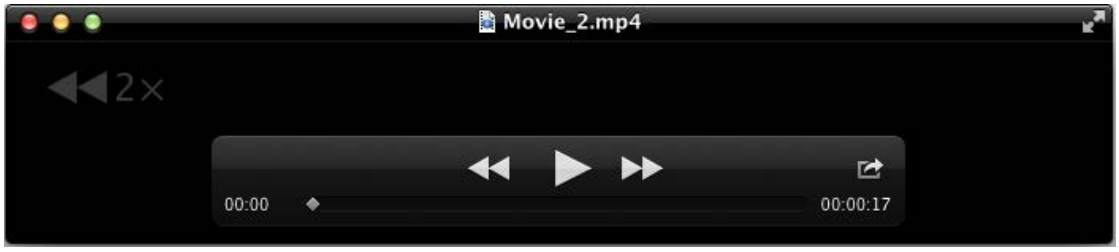

Movie 2

A multi-angle rotational view of GFP positive cell from the dnBMPR1b electroporated cortex at P6 showing random Golgi localization in the cell body.

References:

GUPTA, S. & SEN, J. 2015. Retinoic acid signaling regulates development of the dorsal forebrain midline and the choroid plexus in the chick. *Development,* 142**,** 1293-8.

KAWAKAMI, Y., ISHIKAWA, T., SHIMABARA, M., TANDA, N., ENOMOTO-IWAMOTO, M., IWAMOTO, M., KUWANA, T., UEKI, A., NOJI, S. & NOHNO, T. 1996. BMP signaling during bone pattern determination in the developing limb. *Development,* 122**,** 3557-66.

PHAN, K. D., HAZEN, V. M., FRENDO, M., JIA, Z. & BUTLER, S. J. 2010. The bone morphogenetic protein roof plate chemorepellent regulates the rate of commissural axonal growth. *J Neurosci,* 30**,** 15430-40.